Modeling of Energy Requirements for Fiber Peeling and Mechanical Processing of Hemp

by

Leno José Guzmán Quiñónez

A Thesis submitted to the Faculty of Graduate Studies of

the University of Manitoba

in partial fulfillment of the thesis requirements for the degree of

MASTER OF SCIENCE

Department of Biosystems Engineering

Faculty of Engineering

University of Manitoba

Winnipeg, Manitoba

Canada

General Abstract

The hemp plant is an attractive source of raw material for multiple products. Processing hemp requires the separation of fibre and core components of the plant. Peel tests were conducted for hemp stems to evaluate the strength required to peel fibre from the core. The average peeling force for the Alyssa variety was 0.39 N and that for the USO-14 variety was 0.87 N. The Ising model was implemented to produce a stochastic model. The simulated peel test behaved similarly to the experimental peel test. A discrete element model (DEM) of a planetary ball mill was developed to predict the energy requirement of grinding hemp for fibre. Hemp grinding tests were performed on variety USO-31 using a planetary ball mill for model calibration purposes. Power draw measurements increased linearly increasing at greater grinding speeds. The DEM approximated power draw with relative error below 10% for grinding speeds below 400 rpm.

Acknowledgements

I would like to express my gratitude to my advisor, Dr. Ying Chen, for her support and the excellent guidance that I received throughout my study.

I would like to thank the members of my advisory committee, Dr. Wen Zhong and Dr. Simon Potter, for their helpful advice and comments.

I will also acknowledge Dr. Mashiur Rahman from the Department of Textile Science for allowing me to use the equipment in his laboratory facilities and for providing helpful discussion. I also thank Matt McDonald, Dale Bourns, Robert Lavallee, Derek Inglis, Debby Watson, and Evelyn Fehr for assisting me in various ways during my studies. I will miss you all.

I am grateful for all the incredible support of all my relatives through these challenging times. Finally, I appreciate God Almighty for seeing me through this program.

Dedication

I dedicate this thesis to my parents, Mr. José Guzmán and Mrs. Nuria Quiñónez for their years of guidance and love that motivates me to progress through each day. Thank you for raising me to be who I am today.

Table of Contents

General Abstract ii
Acknowledgements iii
Dedication iv
Table of Contents v
List of Figures vii
List of Tables ix
Chapter 1 Introduction 1
1.1 General 1
1.2 Objectives 2
1.3 Thesis Structure 2
Chapter 2 Literature Review 3
2.1 Hemp Plant 3
2.1.1 General Description 3
2.1.2 Uses of Hemp 4
2.2 Industrial Hemp for Fibre Products 5
2.2.1 Optimizing Yield for Fibre 5
2.2.2 Retting 6
2.2.3 Hemp Decortication 9
2.3 Determination of Hemp Fibre Properties and Behaviour 10
2.3.1 Material Testing 11
2.3.2 Computer Modeling 14
2.4 References 16
Chapter 3 Application of Stochastic Modelling for Simulating Hemp Fibre Peeling Behaviour 23
3.1 Abstract 23
3.2 Introduction 24
3.3 Methodology 28
3.3.1 Peel test 28

3.3.2 Stochastic Model of Fibre Peeling 32
3.4 Results and Discussion 38
3.4.1 Peeling Test 38
3.4.2 Simulation Results 40
3.5 Conclusions 46
3.6 References 46
Chapter 4 Discrete Element Modelling of a Planetary Ball Mill 49
4.1 Abstract 49
4.2 Introduction 50
4.3 Experimental Study 53
4.3.1 Materials and Methods 53
4.3.2 Results and Discussion 55
4.4 Discrete Element Model 58
4.4.1 Model Development 58
4.4.2 Calibration of Damping Coefficient 65
4.4.3 Model Simulations 68
4.5 Conclusion 75
4.6 References 76
Chapter 5 General Conclusions and Recommendations 81

List of Figures

Figure 3.1. Hemp stem cross-section 25
Figure 3.2. Hemp stems used for peeling test. 29
Figure 3.3. Sample preparation: a) Assembly of cutting tool components and b) Prepared hemp stems prior to peeling test. 30
Figure 3.4. Peel test assembly: a) Actual peel test assembly and b) Simplified diagram. 31
Figure 3.5. Sample discretization of fibre and core components (n=20). 33
Figure 3.6. Computer model flow chart. 38
Figure 3.7. Observed behaviour of mechanical test: a) small oscillation range; b) large oscillation range. 39
Figure 3.8. Summary of peeling test results with SD: a) Average peel force and b) Average work to peel. 40
Figure 3.9. Computer model sample output: (a) F=50, U=15, G=20; (b) F=50, U=2, G=20; (c) F=10, U=15, G=20. 41
Figure 3.10. Simulated peeling forces for different scenarios: (a) F=50, U=15, G=20; (b) F=50, U=2, G=20; (c) F=10, U=15, G=20. 43
Figure 3.11. Stochastic model peeling force output. 45
Figure 4.1. Principal components of a planetary ball mill: (a) grinding bowl; (b) grinding balls; (c) relative position of the grinding bowl on the supporting disc. 54
Figure 4.2. Power draw of the planetary ball mill: (a) Effect of grinding speed with samples; (b) Effect of grinding speed without samples. 57
Figure 4.3. The model planetary ball mill at different positions. 59
Figure 4.4. Motion diagram of the planetary ball mil 60
Figure 4.5. Boundary conditions for vector components of the linear velocity. 61
Figure 4.6. Change in velocity components over time at 200 rpm. 62

Figure 4.7. Effect of damping coefficient on power draw at 400 rpm: (a) Ld=0.4, Vd_n=0, Vd_s=0; (b) Ld=0.4, Vd_n=0.3, Vd_s=0.3; (c) Ld=0.4, Vd_n=0.6, Vd_s=0.6. 66
Figure 4.8. Grinding ball motion pattern after one full revolution. 70
Figure 4.9. Velocity distribution of grinding balls at different grinding speeds. 71
Figure 4.10. Total kinetic energy predicted by the model for the 200 rpm grinding speed. 72
Figure 4.11. Average kinetic energy per ball at different grinding speeds. 73
Figure 4.12. Friction power loss at 200 rpm. 74
Figure 4.13. Friction power losses at different grinding speeds. 75

List of Tables

Table 4.1. DEM parameters applied to simulation 64

Table 4.2. Velocity dependent damping coefficients with average relative error of 10%. 68

Chapter 1

Introduction

1.1 General

Modern society is gradually developing towards environmental sustainability. The current level of environmental consciousness has created new expectations about the products that we use in our daily lives. It is no longer acceptable to source raw material for consumer products through non-environmentally-friendly methods. This has created opportunities to reassess current practices and develop alternative product chains that are more environmentally friendly. The re-emergence of a hemp-based product chain is an example of such alternatives becoming more prominent. The hemp plant is a sustainable source of raw material for a wide range of consumer products, including paper, textiles, biocomposites, and food.

Canada started the process of developing the hemp product chain after commercial production of hemp was legalized in 1998. However, the Canadian hemp industry is still facing challenges associated with the lack of detailed technical information. There are multiple ongoing research efforts aiming towards increasing the amount of available technical knowledge relevant to hemp processing. This thesis paper represents one of such efforts and it contains information pertinent to hemp processing.

1.2 Objectives

The primary objective of this thesis was to evaluate mechanical properties of hemp fibre-core separation and approximate these properties through the use of computer modeling tools. The primary objective of this thesis was subdivided into the following specific objectives:

1) Conduct peel tests to evaluate the strength required to separate fibre and core components of hemp stem.
2) Develop a stochastic model that approximates hemp fibre peeling behaviour.
3) Develop a discrete element model to predict the power and energy requirement of grinding hemp for fibre.
4) Approximate stress conditions inside a planetary ball mill via discrete element modeling.

1.3 Thesis Structure

This thesis is structured around two stand-alone papers. A general introduction and literature review are presented in Chapters 1 and 2, respectively. Chapter 3, the first paper, focuses on the development of a stochastic model to simulate the behaviour of a hemp fibre peel test. Chapter 4, the second paper, describes a discrete element model that simulates stress conditions inside a planetary ball mill loaded with hemp stems. Chapter 5 provides general conclusions and recommendations for future research in the area.

Chapter 2

Literature Review

2.1 Hemp Plant

2.1.1 General Description

The hemp plant possesses three key usable components – seeds, core and fibres – with attributes that provide competitive advantages in multiple applications (Brook et al. 2008). Hemp seeds have a diameter of approximately 3 mm, which varies with moisture content of the seed (Sacilik et al. 2003). The bast fibre and core components of the hemp plant are contained within the hemp stalk. Hemp stems are normally 4 – 10 mm in diameter, and hemp plants have a height of 1.5 – 2.5 m (Franck 2005). Core makes up approximately 75% of the hemp stalk (Brook et al. 2008) and it is often referred to as hurd or shive in literature. The total fibre content of hemp stalks is dependent on the plant variety, with values ranging between 15 – 25 % of stalk dry matter. The fibre component of the hemp stalk is composed of several layers of bundles consisting of multiple single fibres. Hemp fibre is categorized based on length and composition; longer fibres contain less lignin and vice versa (Oliver and Joynt 1999).

The average sowing date of the hemp plant in Manitoba is May 25 and the maximum hemp plant height is typically reached by the first to second week of August (Hermann 2008). The hemp plant is a low-input crop since its rapid growth ensures quick canopy closure, providing good natural weed control (Franck 2005;

Baxter and Scheifele 2000; Van der Werf et al. 1996) and therefore avoids the necessity for weed-control chemicals. Hemp has limited fertilizer requirements when compared to other crops (Bennett et al. 2006), such as cotton (Van der Werf et al. 1996), and it has the ability to selectively absorb pollutants, such as heavy metals from soils (Franck 2005). Other detailed information about the physical and chemical characteristics of hemp is available through the work of Bocsa and Karus (1998) as well as Frank (2000) among others.

2.1.2 Uses of Hemp

The market demand for value added products and raw hemp materials are on the rise (Ivanyi 2005). The different components of the hemp plant are processed for use in a wide variety of commercial applications. The hemp seed is extremely nutritious; it is used in foods and nutraceutical products for humans and animals (Vahanvaty 2009; Sherman 2011; Silversides and Lerancois 2005). Hemp oil is suitable for use in industrial products such as paints, varnishes, inks, and industrial lubricants as well as for biodiesel production (Brook et al. 2008). The hemp core is spongy and absorbent, which are ideal characteristics in applications such as animal bedding and industrial absorbents (Gonzales-Garcia et al. 2010). The hemp core is used to produce low-quality paper (Brook et al. 2008) and for the production of building materials such as hemp concrete (Zhijian et al. 2006; Collet and Petrot 2012) and fibreboard (Brook et al. 2008). Hemp bast fibre is used in products where its strength and durability are advantageous, including cordage (rope, twine, etc.), specialty papers, fabrics (clothing and other applications), and

industrial textiles (geotextiles and carpeting) (Brook et al. 2008). The strength of hemp fibre also makes it ideal for use in a range of composite applications such as insulation material or fillers in composites (Brook et al. 2008; Keller et al. 2001).

2.2 Industrial Hemp for Fibre Products

2.2.1 Optimizing Yield for Fibre

Harvesting practices for industrial hemp vary with the purpose of the end products, with some cultivars used for seed only, fibre only, or for dual-purpose production (Hermann 2008). The current thesis focuses on describing practices for optimizing fibre-only production. The fibre morphology and chemistry are influenced by growth stage, age of the plant, and fibre processing (Keller et al. 2001). The work of Mediavilla et al. (2001) describes how fibre yield (the number of primary and secondary fibre cells) depends on the growth stage of the plant (Keller et al. 2001). Primary fibre develops during the phase of rapid stem elongation and consists of large and long fibre cells averaging 20 mm in length. Secondary bast fibre cells are more lignified and shorter, averaging about 2 mm in length (Sankari 2000). Mature hemp stalks produce stronger but stiffer fibres with less elasticity compared to hemp stalks harvested early in the flowering stage (Moes and Empson 2000). Murphy-Bokern and Bruce (2012) collected and processed mature hemp stems into composites. Their study determined that delayed harvest did not affect composite strength; however, composite stiffness was reduced at an approximate rate of 10% per delayed harvest week (Murphy-Bokern and Bruce

2012). In order to minimise the lignification of fibres and maximise the fibre quality, it is considered best to harvest at full flowering for male plants and at the first appearance of flowers for female plants (Struik et al. 2000). Overall, varieties with reduced or delayed onset of lignification are suggested for colder, wetter climates prevalent at northerly latitudes (Bennett et al. 2006).

Seeding rate is another important consideration that affects the physical characteristics of the hemp plant. Hemp is usually seeded at high seeding rates to obtain good weed control due to rapid canopy closure (Baxter and Scheifele 2000). Studies show that high seeding rates promote hemp with thinner stems, resulting in increased fibre yield and quality (Struik et al. 2000; Van Der Werf et al. 1995). Bennett et al. (2006) indicated that proportions of total fibre was higher at the high seeding rate than at the low seeding rate; however, the proportion of long fibre and plant height was unaffected. A decreasing trend of single fibre diameter at higher seeding rates was reported (Amaducci et al. 2008). Khan et al. (2011) linked seeding rate to the tensile strength of hemp fibres; greater seeding rates resulted in increased specific tensile strength.

2.2.2 Retting

Retting is a biological process that removes the pectic substances that bind the fibres to the other constituents of the hemp stalk (Franck 2005). Retting comprises two aspects: the release of the fibre bundles from the core and the separation of the fibre bundles from each other and from the surrounding cortical

tissues (Booth et al. 2004). Processing of hemp fibre can occur in retted or unretted form. The light colour of unretted fibre and low amount of fungal material is considered a marketing advantage (Hobson et al. 2001). Hepworth et al. (2001) determined that fibre produced from unretted stems were coarser but had the same strength as retted stems. Although fibre length depends on the pre-cutting length of the processed straw, retting does affect the length distribution during subsequent processing steps. The decortication processes often result in shortening of hemp fibres; however, the more stable retted fibres are less susceptible to shortening than unretted fibres (Munder et al. 2004). Retting serves the purpose of facilitating the separation of the fibre and core components of the hemp stalk. For high-quality applications requiring longer fibres, the bast fibres should be separated from retted stalks.

Retting is achieved through different methods, including dew, water and chemical retting. Dew retting, also known as ground retting, is the most common type of retting, achieved through placing harvested hemp stalks in the field for up to five weeks. Changes in environmental conditions encourage the growth of microorganisms, which remove the pectin contents (Franck 2005). Water retting is a type of biological retting, similar to dew retting, that accelerates the breakdown of the pectin contents through submerging the stalks in water. Oliver and Joynt (1999) reported that water retting is achievable in a time period of ten days, which is further accelerated through the use of warm water. Chemicals and enzymes are also used for retting. Using this type of technique shortens the retting time

significantly, to about 48 hours, and produces a high quality product (Oliver and Joynt 1999). In Canadian agricultural practice, retting is usually accomplished with dew retting. During dew retting, the freshly harvested stems are initially green, changing to yellow and eventually become almost white. Dew retting is more economical than other types of retting, which is its main advantage; however, dew retting is disadvantageous because it is difficult to control and depends entirely on favourable meteorological conditions (Franck 2005).

If retting timing is appropriate and weather conditions are favourable, there are no adverse changes to the physical properties of the fibre. There are a number of factors affecting the quality of dew-retted fibres. Under ideal conditions, retting is completely selective and does not damage the fibre. In order to avoid damage to the hemp fibre, the duration of retting is critical; under-retting results in fibres that are difficult to separate and process, while over-retting results in damaged fibres that are of little value due to their lower tensile strength (Goodman et al. 2002; Booth et al. 2004; Seaby and Mercer 1985). Seeding rate is also a relevant factor to retting. Bennett et al. (2006) determined that hemp cultivars seeded at lower rates retted more easily and evenly than that from the higher seeding rates; lower seeding rates allow for thinner layers of hemp on the ground during retting (Bennet et al. 2006).

2.2.3 Hemp Decortication

Considerations regarding processing methods are dependent on the ultimate purpose of the material. Decortication of hemp involves the use of mechanical means to separate fibres from the core of the stalk. Commonly used decortication equipment for hemp includes hammer mills and roll crushers. Hammer mills are preferred for applications with unretted hemp where low fibre purity and high processing capacity is required (Chen et al. 2004). Roll crushers are more suitable for retted hemp to produce cleaner and longer fibre. Both decortication methods operate under slightly different principles involving the application of forces to the hemp stem; high impact, shear, and compression forces (Fürll and Hempel, 2000; Gratton and Chen 2004) are individually applied or applied in combination. These types of decortication equipment have problems due to fibre wrapping around rotating parts (Hobson et al. 2001; Dietz 1999); although pre-cutting the hemp stems would alleviate this problem, this is not ideal when long fibres are desirable. Furthermore, this type of equipment is subjected to both energy and productivity inefficiencies. Another alternative has emerged in recent years, which involves the use of ball milling as a decortication method. Previous studies (Baker et al. 2010; Prasad et al. 2005; Khan et al. 2009) evaluated the potential of ball milling as a hemp decorticator. These studies showed how fibre detached from the core due to the impact of the grinding balls inside the mill. Material is placed into a specific size and type of grinding container along with an appropriate size, type, and number of grinding balls (Baker et al. 2010). Overall,

ball mills were able to defibrillate fibrous materials as well as improve fibre quality and fineness through the application of impact and shear forces (Prasad et al. 2005). The main advantage of this decortication method was that fibres were not in contact with any rotating machine parts. Hence, fibre wrapping problems and damage to rotating machine parts are no longer a concern. Further information regarding the use of ball milling for hemp decortication is presented in chapter 4 of this thesis.

2.3 Determination of Hemp Fibre Properties and Behaviour

Man-made fibres, created originally to substitute natural fibres, are today considered inferior to natural fibres in many aspects (Skundric et al. 2008). However, the commercialization of natural fibres, such as hemp fibre products, is currently limited due to inabilities in securing raw materials with consistent material properties and limitations regarding the overall efficiency of the processing equipment. Besides optimized fibre strength, the fibres are required to be as fine and homogeneous as possible (Archibald 1992). There are a variety of research methods that were applied in an effort to enhance the understanding of mechanical properties of different materials, which are also applicable to the study of hemp. The following subsections provide an overview of available techniques to quantify and categorize the mechanics involved in hemp processing.

2.3.1 Material Testing

The most important material properties for technical use of hemp fibres are length, strength, chemical composition, diameter, and surface properties (Hearle et al. 2008). In many applications of hemp fibres, it is required that the fibres perform a load-carrying function. Mechanical testing provides excellent means to determine the effect of different factors on the strength of hemp fibres. Many researchers have determined the breaking tenacity of hemp fibres through tensile tests (Sankari 2000; Khan et al. 2011; Mwaikambo and Ansell 2006; Keller et al. 2001). Other research has focused on the study of the interface between fibre and core components of plant stems (Goodman et al. 2002; Booth et al. 2004). Additionally, the study of surface properties of hemp fibres is also important for fibre use as reinforcements in thermoplastics or concrete composites. There are many techniques available to study the surface properties of hemp, such as fourier transform, infrared spectroscopy, scanning electron microscopy, differential scanning calorimetry, thermogravimetric analysis, gas chromatography, atomic force microscopy, microdroplet single fibre test and pull out tests (Bismark et al. 2002; Mehta et al. 2006; Troedec et al. 2011; Kabir et al. 2012, Eichhorn and Young 2004). All of these analytical tools combined through different research define current efforts to provide a comprehensive investigation of hemp fibre properties.

Breaking tenacity measures strength related to fineness (load per unit fineness) and is directly linked to the fibre tensile strength. Different researchers

focused on the effect of specific factors on the tensile strength of hemp fibre. Research by Kahn et al. (2011) indicated that hemp crop grown with higher plant density should produce finer fibre with higher specific strength and absorb more energy before it ruptures under tensile force. Keller et al. (2001) determined the influence of the hemp growth stage on mechanical properties and concluded that harvesting at the beginning of seed maturity leads to easier decortication without affecting tensile strength. Furthermore, no significant differences between the strengths of different stem sections were found (Keller et al. 2001). Sakari et al. (2000) also reported tenacity and elongation at break, among other properties, of hemp fibres from different plant varieties. The results revealed a marked variation in the breaking tenacity of the fibres even for the same variety and plot. French varieties Fedora 19, Felina 34, and Futura 77 showed significantly higher uniformity than the rest of the studied hemp varieties (Sankari et al. 2000). Overall, the breaking tenacity ranges between 20 and 60 cN/tex (Sankari et al. 2000; Khan et al. 2011).

Mechanical peel tests are generally used to study adhesives bond properties (Hadavinia et al. 2006; Bundy et al. 2000). The mechanical peel test involves the interaction of two components, one being rigid and one being flexible. The components are fixed together with an adhesive and the force required to separate the components is measured to determine the energy bonding them together (Cui et al. 2003). The bond between fibre and core components of plant tissue has similar properties to those studied in adhesives. Peeling tests have been

used to indirectly monitor changes in the mechanical properties of the bond between the fibre and core of flax (Goodman et al. 2002) and hemp stems (Booth et al. 2004). This type of research is able to monitor the effect of factors, such as retting and moisture content, on the amount of energy (work to peel) required to separate fibre and core components of hemp. The direct effect of these factors on the chemical properties of the bond between fibre and core was not monitored.The work to peel was expressed in units of energy per unit area; for hemp, this value ranged from 100 to 400 J m^{-2} (Booth et al. 2004).

It is well known that the performance of composites, in terms of mechanical properties, depends on the properties of the individual components and their interfacial compatibility (Bismark et al. 2002). One of the limitations of using natural fibres in high strength composite applications (biocomposites) is their poor adhesion properties (Kabir et al. 2012). A way to improve the performance of biocomposites is through the use of surface treatments, such as alkalisation, siloxane and acetylation, which enhance adhesion between fibres and matrix (Mehta et al. 2006). Surface modification also results in enhancement of the aspect ratio, improvement in the wettability of the fibres, and the formation of a stronger interface (Mehta et al. 2006). Experimental results by Kabir et al. (2012) found that the hemp fibres processed with surface treatments exhibited better mechanical strength as compared to untreated hemp fibre composite samples (Kabir et al. 2012). Decortication technology is also an important factor affecting the surface properties of natural fibres. In the case of flax fibres, a study performed by Bismark

et al. (2002) presented scanning electron micrographs (SEM) showing differences in the surface morphology, which were dependent on fibre separation processes (Bismark et al. 2002).

Although the above discussion highlights some of the current research efforts related to hemp fibres, there are still missing pieces of information required to optimize the hemp fibre product chain. A deeper understanding of the complex nature of hemp fibres, including their mechanical and surface properties, is still needed in order to identify hemp varieties with more stable fibre quality and less susceptibility to environmental conditions.

2.3.2 Computer Modeling

Computer modeling provides a method to study material behaviour under different scenarios in a controlled environment without the need to perform repetitive experiments. Furthermore, some information derived from computer modeling tools is difficult to obtain through experimental methods. Computing power has increased dramatically over time, which has increased the capacity of computers to realistically represent complex situations. There are many different mathematical tools and computer modeling techniques, which are applicable to the field of hemp processing. However, the focus of this thesis is on the application of two types of models in particular. A stochastic model simulating hemp fibre peeling behavior is described in detail in Chapter 3. A discrete element model (DEM) of a planetary ball mill for hemp grinding is discussed in Chapter 4.

Stochastic models are based on algorithms that rely on random samplings to assist the determination of a result or behaviour. This method is appropriate for simulations involving natural fibres because of the high degree of variation in material properties of hemp. Of particular interest is the application a stochastic algorithm to determine hemp fibre peeling behaviour through the Ising model. The Ising model is a useful tool for the study of stochastic behavior and it has been previously implemented to describe systems (e.g. hemp stalk) consisting of multiple subsystems (e.g. hemp fibre and core). The Ising model is an energy based model that was previously applied in research involving fibre wetting of fibrous assemblies (Zhong et al. 2001), tear behavior of coated fibres (Zhong et al. 2004), fibre debonding during pull out tests and peeling tests (Zhong and Pan 2003). Additionally, the Ising model can potentially approximate the energy bonding fibre and core in hemp plants. Hence, one could study a variety of scenarios involving hemp fibre peeling behaviour in a controlled environment.

The DEM is a computer modeling tool that was used to simulate mechanical behaviours in a variety of research fields, which include mechanical processing scenarios. DEM consists of distinct particles that displace independently of one another and interact only at contacts or interfaces between the particles (Itasca 2008). The DEM time-stepping algorithm requires the repeated application of Newton's second law of motion to each particle inside the considered system. The behavior of particles at each contact is dictated by force–displacement laws and a constant update of particle positions (Rosenkranz et al. 2011). DEM has been

previously applied to model processes relevant to the improvement of hemp fibre processing technologies. Sadek et al. (2011) developed a DEM to simulate the direct shear tests of hemp fibre and core material. The study of the feasibility of processing hemp fibres through different processing methods is possible through DEM. Mishra (2003) and Djordjevic (2003a; 2003b) previously provided detailed explanations about the modeling of ball milling equipment through DEM. Similarly, simulation of other types of processes could provide detailed information about stress conditions during hemp processing that would otherwise not be available through other experimental methods.

2.4 References

Amaducci S., A. Zatta, F. Pelatti and G. Venturi. 2008. Influence of agronomic factors on yield and quality of hemp (Cannabis sativa L.) fibre and implication for an innovative production system. Field Crops Research 107(2): 161-169

Archibald, L.B., 1992. Quality in flax fibre. In: Shekhar Sharma, H.S., Van Sumere, C.F. (Eds.), The Biology and Processing of Flax. M. Publications, Belfast, pp. 297–309.

Baxter, W.J. and G. Scheifele. 2000. Growing Industrial Hemp in Ontario. Ministry of Agriculture and Food, Ontario.

Bennett, S. J., R. Snell and D. Wright. 2006. Effect of variety, seed rate and time of cutting on fibre yield of dew-retted hemp. *Industrial Crops and Products*. 24:79-86.

Bismark, A., I. Aranberri-Askargorta, J. Springer, T. Lampke, B. Wielage, A. Stamboulis, I. Shederovich and H. Limbach. 2002. Surface Characterization of Flax, Hemp and Cellulose Fibers; Surface Properties and the Water Uptake Behavior. Polymer Composites 23(5):872-894.

Bocsa, I. and Karus, M. 1998. The Cultivation of Hemp: Botany, Varieties, Cultivation and Harvesting. Hemptech, Sebastopol, CA.

Booth I., A.M. Goodman, R.J. Harwood and S.A. Grishanov. 2004. A mechanical investigation of the retting process in dew-retted hemp (Cannabis sativa). *Annals of Applied Biology*.145 (1):51-58.

Brook G., K. Liljefors, D. Brook, and A. Stewart. 2008. National industrial hemp strategy. Prepared for: Manitoba Agriculture, Food and Rural Initiative (summited 2008 03 30). 358 p.

Bundy, K. 2000. An improved peel test method for measurement of adhesion to biomaterials. Joural of Material Science: Materials in Medecine. 11:517-521.

Chen, Y., J. Lui and J. L. Gratton. 2004. Engineering perspective of Hemp Plant, Harvesting and Processing: A Review. Journal of Industrial Hemp 9(2):23-39.

Collet, F., S. Pretot. 2012. Experimental investigation of moisture buffering capacity of sprayed hemp concrete. Construction and Building Materials 36: 58-65.

Cui, J., R. Wang, A. N. Sinclair and J. K. Spelt. 2003. A calibrated finite element model of adhesive peeling. *International Journal of Adhesion & Adhesives*. 23:199-206.

Djordjevic, N. 2003a. Discrete element modelling of the influence of lifters on power draw of tumbling mills. Minerals Engineering 16(4):331-336.

Djordjevic, N. 2003b. Discrete element modelling of power draw of tumbling mills. Mineral Processing and Extractive Metallurgy 112(2):109-114.

Eichhorn, S. J. and R. J. Young. 2004. Composite micromechanics of hemp fibres and epoxy resin microdroplets 64(5):767-772.

Franck R. R. 2005. Bast and other plant fibres. Textile Institute. Manchester, England. CRC Press LLC. 397 p.

Gonzales-Garcia, S., A. Hospido, G. Feijoo and M. T. Moreira. 2010. Life cycle assessment of raw materials for non-wood pulp mills: Hemp and flax. Resources, Conservation and Recycling 54(11): 923-930.

Goodman A. M., A. R. Ennos and I. Booth. 2002. A mechanical study of retting in glyphosate treated flax stems (Linum usitatissimum). Industrial Crops and Products 15 (2):169-177.

Gratton, J.L. and Y. Chen. 2004. Development of a field-going unit to separate fibre from hemp (Cannabis sativa) stalk. Applied Engineering in Agriculture 20(2):139-145.

Hadavinia H., L. Kawashita, A. J. Kinloch, D. R. Moore and J. G. Williams. 2006. A numerical analysis of the elastic-plastic peel test. *Engineering Fracture Mechanics* 73 (16):2324-2335.

Hearle, J. W. S and W. E. Morton. 2008. Physical Properties of Textile Fibres, 4th ed. Textile Institute. Manchester, England. The textile institute. 776 p.

Hermann, A. M. 2008. The Effect of Plant Population Density and Harvest Timing on Agronomic Fibre Yield and Quality Characteristics of Industrial Hemp (Cannabis), Cultivar Alyssa, Grown in the Parkland Region of Manitoba, Canada. Unpublished. M. Sc. Thesis. Winnipeg MB: Department of Plant Science, University of Manitoba.

Hobson R. N., D. G. Hepworth and D. M. Bruce. 2001. Quality of Fibre Separated from Unretted Hemp Stems by Decortication. Journal of Agricultural Engineering Research 78(2):153-158.

Itasca. 2008. PFC3D particle flow code in 3 dimensions, theory and background. Minneapolis, Minnesota, USA: Itasca consulting group, Inc.

Kabir, M. M., H. Wang, K. T. Lau, F. Cardona and T. Aravinthan. 2012. Mechanical properties of chemically-treated hemp fibre reinforced sandwich composites. Composites Part B: Engineering 43(2):159-169.

Khan, M. R., Y. Chen, O. Wang and J. Raghavan. 2009.Fineness of Hemp (Cannabis Sativa L.) Fiber Bundle after Post-Decortication Processing Using a Planetary Ball Mill. Applied Engineering in Agriculture 25(6):827-834.

Khan, M. R. K., Y. Chen, T. Belsham, C. Lague, H. Landry, Q. Peng and W. Zhong. 2011. Fineness and tensile properties of hemp (Cannabis sativa L.) fibres. Biosystems Engineering 108(1): 9-17.

Keller, A., M. Leupin, V. Mediavilla and E. Wintermantel. 2001. Influence of the growth stage of industrial hemp on chemical and physical properties of the fibres. *Industrial Crops and Products*. 13:35-48.

Mehta, G., L. T. Drazal, A. K. Mohanty and M. Misra. 2006. Effect of Fiber Surface Treatment on the Properties of Biocomposites from Nonwoven Industrial Hemp Fiber Mats and Unsaturated Polyester Resin. Journal of Applied Polymer Science 99(3):1055-1068.

Moes, J. and Empson, W. 2000. Preliminary study of hemp fibre properties. Emerson HempCompany.

Munder, F., C. Furll and H. Hempel. 2004. Advanced Decortication Technology for Unretted Bast Fibres. Journal of Natural Fibres 1(1): 49-65.

Murphy-Bokern, D. and D. M. Bruce. Research and development final report: Properties of fibre extracted from unretted hemp and fibre performance in composites. Silsoe Research Institute, Wrest Park, Silose, Bedford shire, Mk45 4HS http://www.ienica.net/usefulreports/fibre.pdf 29-10-2012.

Mwaikambo, L. Y. and Ansell, M. P. 2006. Mechanical properties of alkali treated plant fibres and their potential as reinforcement material: 1 hemp fibres. Journal of Material Science. 41:2483-2496.

Oliver, A. and H. Joynt. 1999. Industrial Hemp Fact Sheet. British Columbia Ministry of Agriculture and Food. Kamloops, British Columbia. 20.

Rosenkranz S., S. Breitung-Faes and A. Kwade. 2011. Experimental investigations and modelling of the ball motion in planetary ball mills. Powder Technology. 212:224-230.

Sadek, M. A., Y. Chen, C. Lague, H. Landry, Q. Peng and W. Zhong. 2011. Characterization of shear properties of hemp fiber and core using the discrete

element model. Transactions of the American Society of Agricultural and Biological Engineers 54(6):2279-2285.

Sacilik, R., R. Ozturk and R. Keskin. 2003. Some physical properties of hemp seed. Biosystems Engineering 86(2):191-198.

Sankari, H. S. 2000. Comparison of bast fibre yield and mechanical fibre properties of hemp (Cannabis sativa L.) cultivars. Industrial Crops and Products 11(1): 73-84

Seaby, D. A. and P. C. Mercer. 1985. A hand tool to assess the strength of flax and other fibrous materials. Annals of Applied Biology. 106: 205-210.

Sherman, L. 2011. Hemp Seed Pill eases constipation. The Journal of Chinese Medicine (95): 74.

Silversides, F. G. and Lefrancois, M. R. 2005. The effect of feeding hemp seed meal to laying hens. British Poultry Science 46(2):231-235.

Skundric, P., B. Pejic, and M. Kostic. 2008. Quality of chemically modified hemp fibres. *Bioresource Technology*. 99:94-99.

Struik, P. C., S. Amaducci, M. J. Bullard, N. C. Stutterheim, G. Venturi and H. T. H. Cromack. 2000. Agronomy of fibre hemp (Cannabis sativaL.) in Europe. Industrial Crops and Products. 11(2-3):107–118.

Troedec M., A. Rachini, C. Peyratout, S. Rossignol, E. Max, O. Kaftan, A. Fery and A. Smith. 2011. Influence of chemical treatments on adhesion properties of hemp fibres. Journal of Colloid and Interface Science 356(1):303-310.

Vahanvaty, U. S. 2009. Hemp Seed and Hemp Milk: The New Super Foods?. Infant, Chlid, & Adolescent Nutrition 1(4): 232-234.

Van Der Werf, H.M.G., M. Wijlhuizen, J. A. A. De Schutter. 1995. Plant density and self-thinning affect yield and quality of fibre hemp (Cannabis sativaL.). Field Crops Research. 40(3):153–164.

Van Der Werf, H. M. G, A. J. Haverkort and E. W. J. M. Mathussen. 1996. The potential of hemp (Cannabis sativa L.) for sustainable fibre production: a crop physiological appraisal. Annals of Applied Biology. 129:109-123.

Zhijian, L., X. Wang and L. Wang. 2006. Properties of hemp fibre reinforced concrete composites. Composites Part A: Applied Science and Manufacturing 37(3): 497-505.

Zhong W. and N. Pan. 2003. A Computer Simulation of Single Fiber Pull Out Process in a Composite. Journal of Composite Materials 37(21): 1951-1969.

Zhong W., N. Pan and D. Lukas. 2004. Stochastic modelling of tear behaviour of coated fabrics. Modelling and Simulation in Materials Science and Engineering 12(2): 293-309.

Zhong, W., X. Ding, Z. L. Tang. 2001. Modeling and Analyzing Liquid Wetting in Fibrous Assemblies. Textile Research Journal 71(9):762-766.

Chapter 3

Application of Stochastic Modelling for Simulating Hemp Fibre Peeling Behaviour

3.1 Abstract

The separation of fibre and core components of hemp stems is a fundamental step in hemp decortication, mechanical separation of fibre and core. This research aimed to enhance the understanding of fibre-peeling behaviour of hemp to improve the current decortication technologies. Peel tests were conducted for hemp stems to evaluate the strength required to peel fibre from the core. The peel tests were performed on retted and unretted hemp samples under each of two hemp varieties, USO 14 and Alyssa. Results showed that force and work required to peel did not vary with the retting condition, but with the hemp variety. This was possibly a consequence of under-retting of the hemp stems due to unfavourable environmental conditions. The average peeling force for the Alyssa variety was 0.39 N and that for the USO 14 variety was 0.87 N. Within the Alyssa variety, the work required to peel the fibre from the core was 193 J m^{-2}, and the work required to peel the fibres of the USO 14 variety was 431 J m^{-2}. The Ising model was implemented to produce a stochastic model which simulated the peeling force obtained from the peel tests. The behaviour of the simulated peel test was similar to that observed during the peel test and the process of fibre peeling was successfully simulated through the use of a stochastic algorithm. The

stochastic model simulated the average peel force to be 0.86 N for the USO 14 variety and 0.39 N for the Alyssa variety.

Keywords: stochastic model, hemp, peel, debonding, fibre, core, force, work

3.2 Introduction

There is increasing interest from many potential end-users of hemp-based products, especially hemp fibre (Brook et al. 2008). Hemp (*Cannabis sativa* Linnaeus) fibres are among the strongest natural sources of fibre, which is a desirable characteristic in applications such as bio-composites and textiles. Mechanical separation of fibre from the hemp stem is a fundamental step in hemp processing for fibres. The cross-section of hemp stem is illustrated in Figure 3.1. The outer layer is known as the cortex, which is the thin protective layer containing chlorophyll. The phloem layer consists of chlorophyll-containing short cells as well as long cells known as the bast fibres. These two layers combine to form the fibre component of the hemp stem. Hemp produces phloem fibres which are cemented into place by a complex mixture of pectins, hemi-celluloses and lignin (Booth et al. 2004). The cambium layer is also known as the fibre-core interface layer, where fibre and core debond during mechanical separation. The pith layer provides structural support and can be identified as the core of the plant. The hemp stem possesses a hollow centre through its length, with the exception of the joints between internodes. In modeling of mechanical properties of hemp in this study, the hollow structure of hemp stem is considered to have only two distinct components: fibre and core.

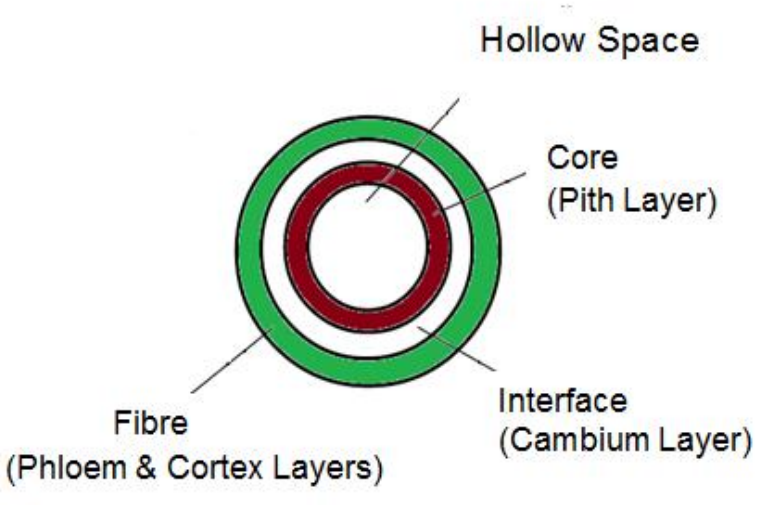

Figure 3.1. Hemp stem cross-section (the proportions of the layers are not to scale)

The process of mechanically separating fibre and core is commonly known as decortication. Decortication requires the use of machinery such as hammer mills and roll crushers. Current decortication machines are not energy efficient and yield low purity product (Baker 2009) due to lack of the knowledge about the mechanical properties of hemp. Energy requirement and effectiveness of the decortication process depends on the adhesive energy bonding fibre and core together. Therefore, understanding the bonding strength between fibre and core is essential for the design and improvement of decortication processes.

Mechanical peel tests are generally used by engineers to study adhesives (Hadavinia et al. 2006; Bundy et al. 2000) and are implemented to investigate the separation of plant tissues (Goodman et al. 2002; Booth et al. 2004). The mechanical peel test consists of two adherents, one being rigid and one being

flexible, which are fixed together with an adhesive. Once the elements are combined, the force required to separate the adherents is measured to determine the adhesive energy bonding them together. Booth et al. (2004) used a mechanical peel test in hemp stems to investigate factors that affect the work to peel, including peeling angles, moisture content and retting; the results provided insight on the comparability of peel tests performed under combinations of the previously mentioned factors.

Retting may precede decortication to reduce the energy required for decortication and minimize the fibre breakage during decortication. Retting is a biological process that encourages the removal of the pectic substances that bind the fibre to the core. In Canadian agricultural practice, retting is usually achieved by ground retting. During ground retting, hemp plants are laid in swathes on the ground as they are harvested. The combined action of dew and showers of rain provide the necessary conditions for the development of the microorganisms on the stems (Franck 2005).

The process of peeling hemp fibre from the core is subjected to oscillations in the peeling force (Booth et al. 2004), as observed during peel tests of other materials (Inoue and Sugannuma 2009; Von Maubeuge and Ehrenberg 2000; Xie and Karbari 1998). The oscillations of the peel force are a product of the adhesive's properties, which can be described as stochastic in nature. The Ising model is a useful tool for the study of stochastic behaviour. The Ising model was

introduced as a mathematical model to describe ferromagnetism in statistical mechanics and it is often used to study systems consisting of multiple interactive subsystems (Yeomans 1992). The macro characteristics of the system are represented as interactions and resulting balances among the micro characteristics of subsystems present in the model. Energy based models, such as the Ising model, serve as a tool to describe stable debonding of long embedded fibres (Zhong and Pan 2003), which is comparable to the removal of hemp fibre from the core. The processes were simplified as systems consisting of the interaction of subsystems with two interchangeable states (Zhong et al. 2001; Zhong and Pan 2003; Zhong et al. 2004). Of particular interest is the work of Zhong and Pan (2003), which discusses the simulation of a hypothetical single-fibre-peel process of a polymer with half of its volume embedded lengthwise in a block of cured matrix. One of the advantages of the presented method is its applicability to describe such phenomena as partial debonding, fibre breaking, and matrix failure; these phenomena are difficult to deal with using other existing methods (Zhong and Pan 2003).

The objectives of this study were to (1) conduct peel tests to evaluate the strength required to separate the hemp fibre-core interface and (2) to develop a stochastic model to predict the peeling strength of hemp fibre using the Ising model.

3.3 Methodology

3.3.1 Peel test

3.3.1.1 Experimental Design

The peel test was performed on two hemp varieties, USO 14 and Alyssa, from crops grown in Manitoba, Canada. At the normal harvest time, hemp plants were manually harvested at different random locations of the field. For each variety, half of the plants were retted and the other half remained unretted. Retting was achieved by leaving hemp plants in the field for a period of three weeks. Having two varieties and two retting conditions resulted in a total of four different treatments. Twenty samples were tested for each treatment, giving a total of 80 peel tests.

3.3.1.2 Sample Preparation

The average moisture content of unretted and retted samples was 7.5%. Samples were prepared in a multiple-step process. The first step was to cut hemp stems into segments of 100 and 150 mm in length (Figure 3.2). The sample length was chosen in accordance to the distance between internodes within the hemp stems. The segments were taken from different regions of hemp stem. The average diameter of the segments was 8.5±1.3 mm for Alyssa variety and 12.6±2.8 mm for USO14. Cutting was done using an exacto knife to cut around the outer layers of the stem and using a small metal saw to cut the inner core of the stem. This prevented damage to the fibre-core interface prior to the peel test. The

second step was conditioning the samples in an environmental chamber for seven days at 21ºC and 40 % relative humidity prior to the peel test.

Figure 3.2. Hemp stems used for peeling test.

The final step was making a cut along the major axis of each sample, ensuring a constant width of 2 mm for each peel as the test was performed. The cutting tool was composed of two blade tips extracted from an exacto knife and a grip (Figure 3.3a). The blades were separated by a piece of metal that provided the 2-mm distance between the blades. The 2-mm distance in combination with the peel force is also used as a means to determine the work required to peel. After the cutting tool was used to prepare the sample for peeling, a transverse cut was made to manually initiate separation of the fibre from the core (Figure 3.3b).

The peeled fibre was consistently clamped to the upper grip at a distance of 20 mm away from the stem.

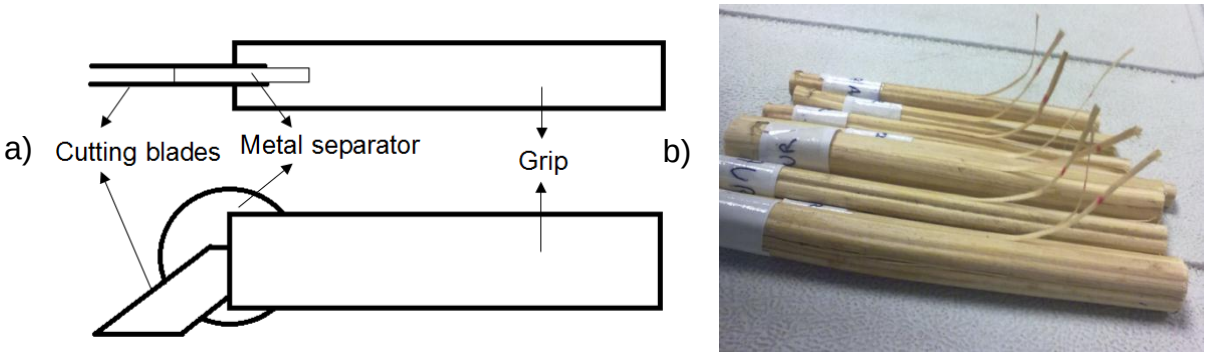

Figure 3.3. Sample preparation: a) Assembly of cutting tool components and b) Prepared hemp stems prior to peeling test.

3.3.1.3 Testing Procedure

The implemented procedure followed a combination of methods introduced by ASTM standards (ASTM 2004) and the work described by Booth et al. (2004). A universal test frame was used for the peel tests (Figure 3.4a). The test frame was an Instron 5965 equipped with a 5-N load cell. Figure 3.4b further illustrates the setup of the peel test assembly. A long (300-mm) non-extensible string was used to maintain relatively constant peeling angle, 90º ± 3º, as the peeling action was extended during the test. Booth et al. (2004) reported that peeling angles of 90º ± 15º would not significantly affect the work to peel hemp fibre from the core. A bulldog clip was added to the extension piece to facilitate the attachment of the fibre to the upper fixture. The rate of extension of the upper fixture was 40 mm min^{-1}. The effective peeling distance was 20 mm for each sample. The use of this

assembly resulted in minimum change in peeling angle, while allowing the use of simple screw side-action grips to attach the samples to the test frame. The lower fixture kept the stem in a fixed horizontal position with the aid of rubber attached to its surface. The contact point between the bulldog clip and the fibre was coloured with ink to ensure that any slippage would be detected and the test was discarded if necessary.

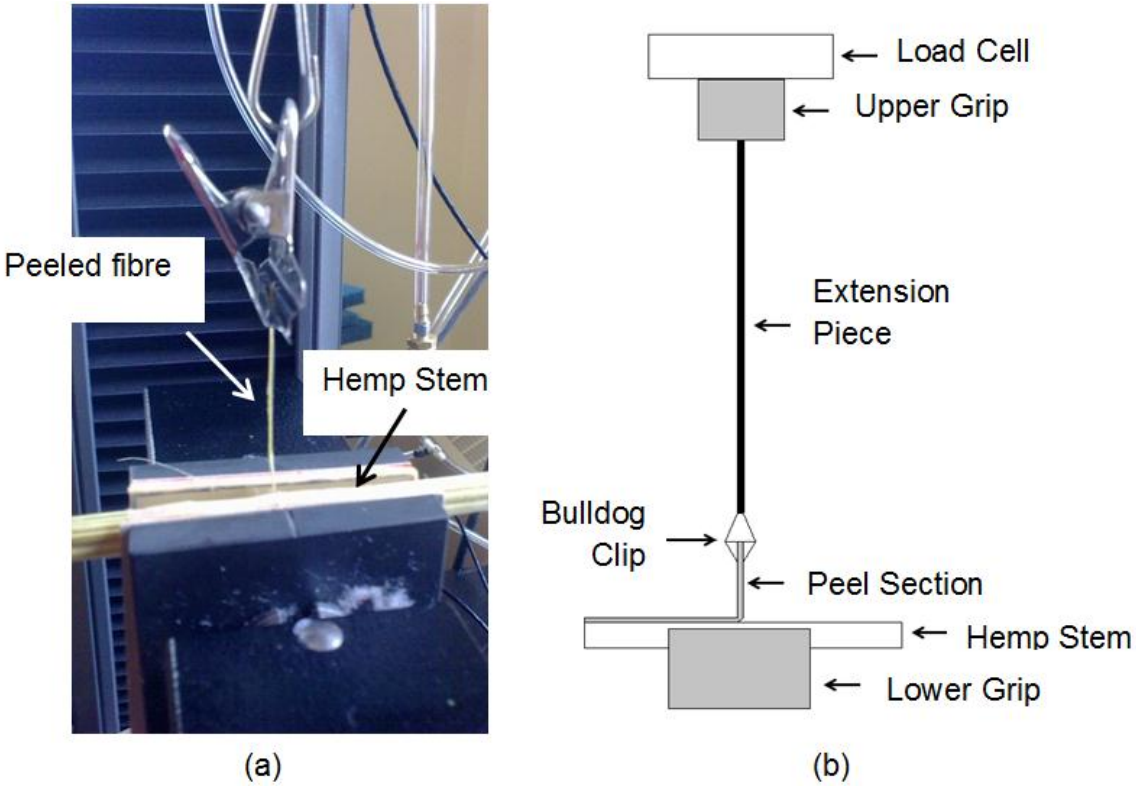

Figure 3.4. Peel test assembly: a) Actual peel test assembly and b) Simplified diagram.

3.3.1.4 Measurements and Data Analysis

The force against displacement data from the peel test were collected with an interfaced computer. The average peeling force was determined as the

average of the peel force between 5 and 15 mm of displacement expressed in N, which ensured that the peeling force had stabilised after the characteristic initial peak in force. The work required to peel the fibre from the core was equivalent to the total work divided by the area of peel exposed and was expressed in J m^{-2}. The data was examined using an analysis of variance fitted to a generalized linear model (GLM) of the Statistical Analysis System (SAS 9.1) computer package.

3.3.2 Stochastic Model of Fibre Peeling

The application of two mathematical principles, the Ising model and a Monte Carlo simulation, dictated the overall behavior of the stochastic model. The Ising model defined the distribution of the internal energy of the modeled hemp stem. The proposed model scenarios – including fibre breaking, fibre debonding, and core pull-out – were based on the energy difference between each change in state. The Monte Carlo simulation had the capacity of appropriately determining which scenario will manifest itself during the peeling process. Detailed information regarding the application of these mathematical principles for the proposed model is outlined in the following subsections.

3.3.2.1 Energy Balance Determination

The fibre and core components were represented by the Ising model as subsystems bearing two interchangeable configurations, bonded or debonded, between adjacent components. The components of the system were discretized as cells representing individual subsystem regions. The position of the subsystem

regions was arranged in a two-dimensional structural framework. Figure 3.5 represents the cross-section of a hemp stem along the axial direction, where the state of Individual cells was stored in an *nxn* matrix in which *n* was equal to 20. The arrangement of the actual system was assigned an *n* value equal to 400 to increase the resolution of the model as well as to provide enough peeling length later on the model. The cells within the proposed system could be filled with three possible states; empty, filled by fibre or filled by core. However, fibre and core shall not simultaneously occupy any individual cell at any given time. In the current model, the light gray cells represent the fibre component and the dark gray cells represent core component.

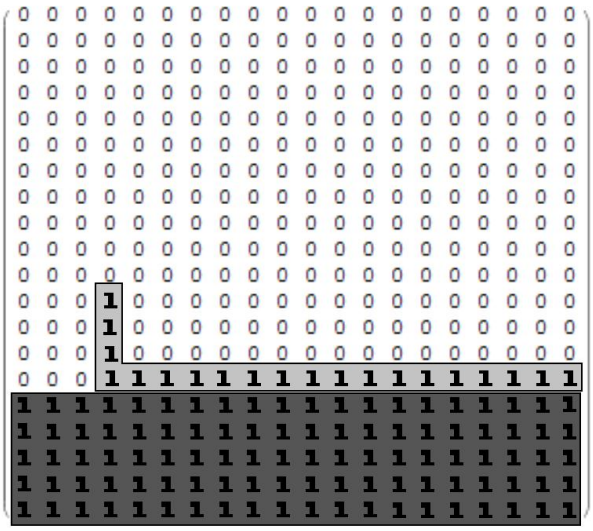

Figure 3.5. Sample discretization of fibre and core components (n=20).

The model incorporates three important properties involved during the peeling process: the tensile strength of the fibre, the strength of the core, and the

strength of the fibre-core interface. The change in the internal energy (*dE*) of the system was described as:

$$dE = \sum e_i \, dm_i \; + \sum m_i \, de_i = dH + W \tag{1}$$

where e_i is the internal energy of given cell i, m_i is the number of subsystem having internal energy e_i, *dH* is the change in the Hamiltonian, and *W* is the extrinsic work done to the system. The internal energy of the system can be altered by either the change of state of e_i or the rearrangement of m_i during the peeling process. The Hamiltonian, *dH*, represents the summation of the interactions between each cell and its nearest neighbours. The change in energy due to extrinsic work (*W*) done to the system is representative of the applied peeling force.

This configuration resulted in a total of four variables capable of describing the state of each cell. (i) F_i = Cell *i* is occupied by fibre ($F_i = 1$) or not ($F_i = 0$). (ii) f_i = Fibre cell *i* is bonded to the core ($f_i = 1$) or not ($f_i = 0$). (iii) C_i = Cell *i* is occupied by core ($C_i = 1$) or not ($C_i = 0$). (iv) c_i = Core cell *i* is bonded to adjacent core ($c_i = 1$) or not ($c_i = 0$). The energy of the system (*H*) can be expressed for each single cell i as:

$$H = -T \sum_{j}^{cn} F_i F_j S_{ij} - U \sum_{j}^{cn} C_i C_j S_{ij} - G \sum_{j}^{ct} (f_i c_j + c_i f_j) S_{ij} \tag{2}$$

where the first term in the right hand side of Eq. 2 represents the tensile strength of the hemp fibre, where: *T* denotes the cohesive energy between each connecting

fibre cell, *cn* denotes the sum of the *F* value over all the fibre cells connected to cell *i*, and S_{ij} accounts for the interaction area between cells *i* and *j*. The second term denotes the strength of the core, where *U* is representative of the cohesive energy between each connecting core cell. In this term, *cn* denotes the sum of the *c* values over all of the core cells in connection to cell *i*. The last term denotes the fibre-core interface, where *G* reflects the adhesive energy between the fibre and the core and *ct* denotes the sum of *c* or *f* values of the cells in contact with cell *i*. It is important to note that if a given cell *i* is occupied by fibre, which is bonded to the core, only the first term inside the brackets has nonzero values. Similarly, if the given cell *i* is occupied by core, which is bonded to the fibre, only the second term inside the brackets has nonzero values. Another feature shown in Eq. 2 is the fact that *G* is no longer in effect after debonding from the fibre cell occurs (f = 0).

The expression for the interaction area, S_{ij}, is determined under the assumption that fibres are shaped as cylinders. The diameter of each fibre bundle is approximated to be 0.15 mm (Kahn et al. 2010). The interaction area at the fibre-core interface was modelled as half the surface area of a cylinder with both diameter and length equal to the fibre diameter *d*. Interaction areas at connecting fibre-fibre or core-core cells were modelled as circles of diameter *d*. These interaction areas were then multiplied by the number of fibre bundles to account for the peel thickness. The number of fibre bundles per peel, *b*, is a unitless constant determined by both the approximate diameter of the bundles and the peel. The

width of the peeled fibre is 2 mm. Therefore, the value of *b* was equal to 13.3 fibre bundles per peel.

$$S_{ij} = \begin{cases} b\frac{\pi d^2}{2} & \text{(cell } i \text{ is above or below cell } j\text{)} \\ b\frac{\pi d^2}{4} & \text{(cell } i \text{ is directly connected to cell } j\text{)} \end{cases} \quad (3)$$

3.3.2.2 Fibre Peeling Simulation

The most common change in state for this particular simulation is likely to be dictated by the energy difference before and after fibre debonding. A debonding fibre cell, *i,* is represented by a fibre cell which has changed from a bonded state (f_i=1) to a debonded state (f_i=0). The expression for the energy difference can be written as:

$$\Delta E = H_2 - H_1 - Rd \quad (4)$$

where H_1 and H_2 represent the internal energy of the system at different states, *R* is the peeling force, and *d* is the diameter for each step. The product of *R* and *d* is the work done to the system by peeling force.

Using the Monte Carlo method requires calculations to rely on repeated random saplings to determine the outcome of the model. Each step in the calculation of energy difference, for a given cell i, involves the use of a probability distribution. The probability, *P*, of change in the system from one state to another is calculated by using the Metropolis function (Yeomans 1992) given by:

$$P(E_2|E_1) = \min\left[1, e^{\left(\frac{-\Delta E}{\beta}\right)}\right], \qquad (0 < P \leq 1) \qquad (5)$$

where *P* is given a value of 1 when $\Delta E = E_2 - E_1 \leq 0, or\ E_2 \leq E_1$. This means that changes from higher energy states to lower energy states have a definite probability of occurring. In the opposite situation, whenever $E_2 > E_1$, *P* falls somewhere within $0 < P < 1$. A random number *r*, which is uniformly distributed and falls between zero and one, is selected and the state change occurs only if $r < P$. The previously described arrangement implies that the internal energy difference ΔE at any possible state change scenario is always positive and therefore, quite unlikely to occur spontaneously. As a consequence of this, a sufficient amount of extrinsic work is required to counteract the positive internal energy difference and produce a probability *P* which is large enough to generate a state change. The effect of thermal perturbation is reflected by the thermodynamic constant, β, and is assigned a constant value of 0.008 at room temperature. This value could be adjusted to account for thermal fluctuations, but the contribution of thermal energy to the current simulation is insignificant. Figure 3.6 summarizes flow of the main modules of the implemented simulation program.

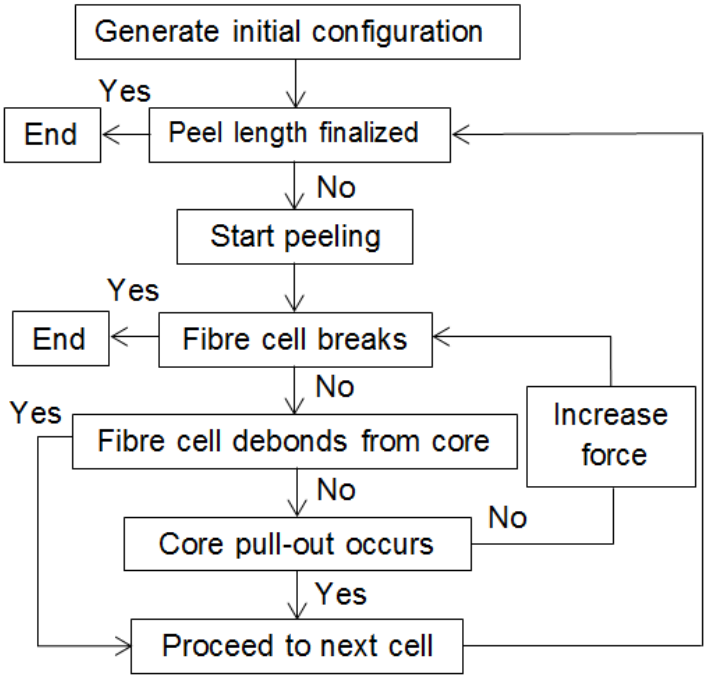

Figure 3.6. Computer model flow chart.

3.4 Results and Discussion

3.4.1 Peeling Test

3.4.1.1 Force Displacement Curves

The oscillation patterns of the peel force versus displacement curves varied for all samples independently of hemp variety and retting conditions. Most samples of both varieties behaved in a similar pattern but varied in the magnitude of the average peeling force. The peeling force reached a peak value approximately between 0 and 5 mm of displacement. Subsequently, the load oscillated about an average value until the test was completed. The load oscillations varied in their range for the different samples; some samples produced

curves with fairly small oscillations about the average value of the peel force, as shown in Figure 3.7a, while the other observed oscillation behaviour consisted of larger oscillations about the average value of the peel force, as observed in Figure 3.7b.

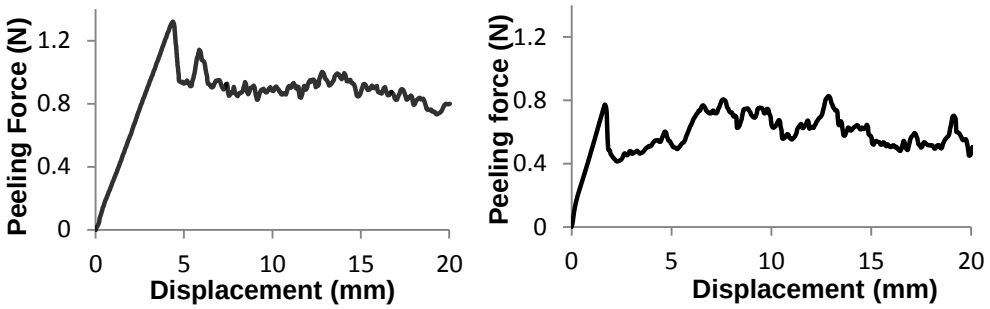

Figure 3.7. Observed behaviour of mechanical test: a) small oscillation range; b) large oscillation range.

3.4.1.2 Peeling Force and Work

Results for each hemp variety showed that the peeling force was significantly different from one another (Figure 3.8a). However, retting for a period of three weeks did not yield significantly different peeling force when compared to the samples that were unretted. The average peeling force for the Alyssa variety was 0.37 ± 0.25 N and 0.41 ± 0.23 N for unretted and retted samples, respectively. The USO 14 variety had larger average peeling forces, with values of 0.86 ± 0.51 N for unretted samples and 0.87 ± 0.59 N for retted samples. Similarly, the peeling work was significantly different between the hemp varieties, but not between the retting conditions (Figure 3.8b). Within the Alyssa variety, the work required to peel

the fibre from the core was 183 ± 126 J m^{-2} for unretted samples and 203 ± 117 J m^{-2} for retted samples. The work required to peel fibres of the USO 14 variety had minimal differentiation between two retting conditions, resulting in 428 ± 256 J m^{-2} and 433 ± 292 J m^{-2} for unretted and retted samples, respectively. This range of values was comparable to those obtained by Booth et al. (2004), who obtained values ranging between 100 and 400 J m^{-2} through a similar experiment.

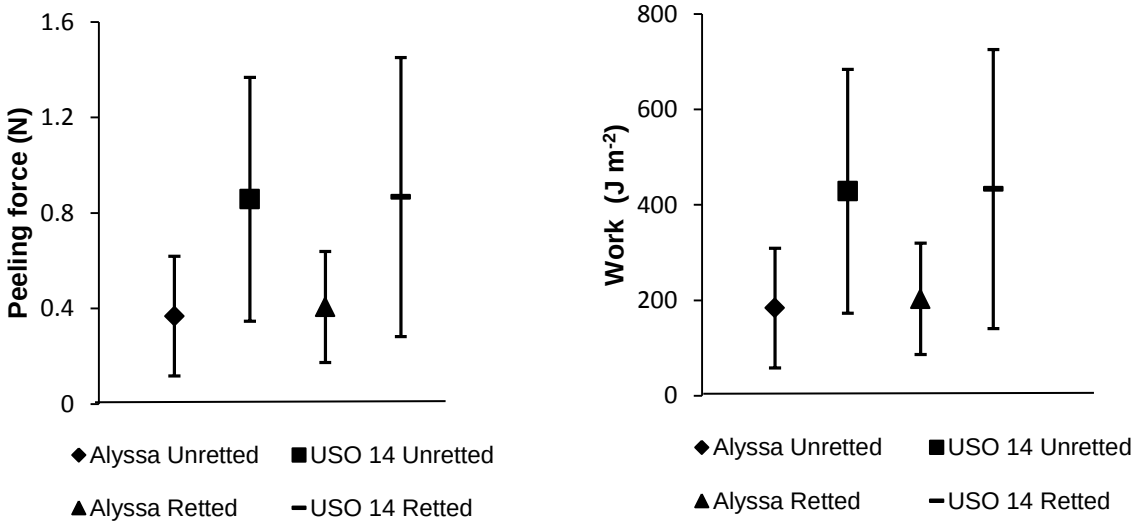

Figure 3.8. Summary of peeling test results with SD: a) Average peel force and b) Average work to peel.

3.4.2 Simulation Results

3.4.2.1 Model Behaviour

Preliminary tests were performed on the model to determine whether the simulation was behaving as expected. Figure 3.9 shows the results of the test

when using different magnitudes for the coefficients of the internal energy constants of F, U and G. For scenario (a), the fibre and core were strong enough to allow for clean peeling. For scenario (b), the fibre-core interface is significantly stronger than the cohesive energy of the core-core interface, which resulted in some of the core material to be peeled off in conjunction with the fibre. For scenario (c), the fibre itself was too weak to withstand peeling, which resulted in the fibre breaking before the peeling could occur. The model behaved as expected for each scenario.

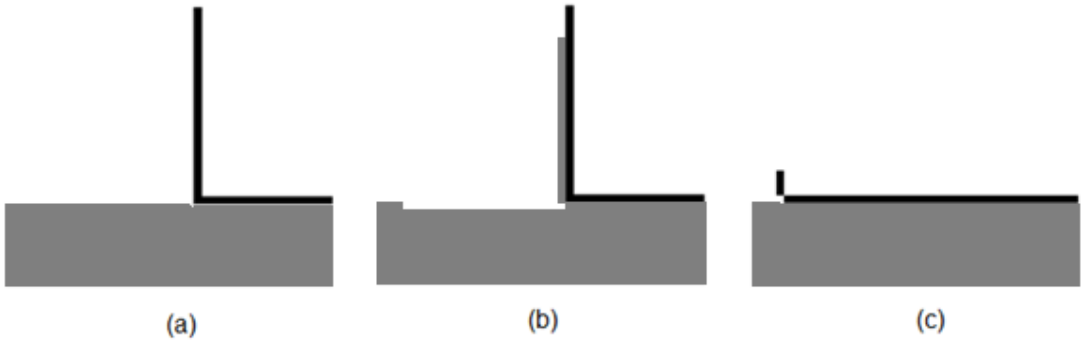

Figure 3.9. Computer model sample output: (a) F=50, U=15, G=20; (b) F=50, U=2, G=20; (c) F=10, U=15, G=20.

3.4.2.2 Simulated Peeling Force

The peeling force versus displacement curves for each scenario are shown in Figures 3.10a, b and c. The output for scenario (a) produced load oscillations about an average value, which behaved similarly to a mechanical peel test. The output for scenario (b) was similar to (a), but the magnitude of the average value of

the peeling force was larger than the one observed in scenario (a). Scenario (c) shows how the peeling force increased until the fibre broke and no force was recorded afterwards.

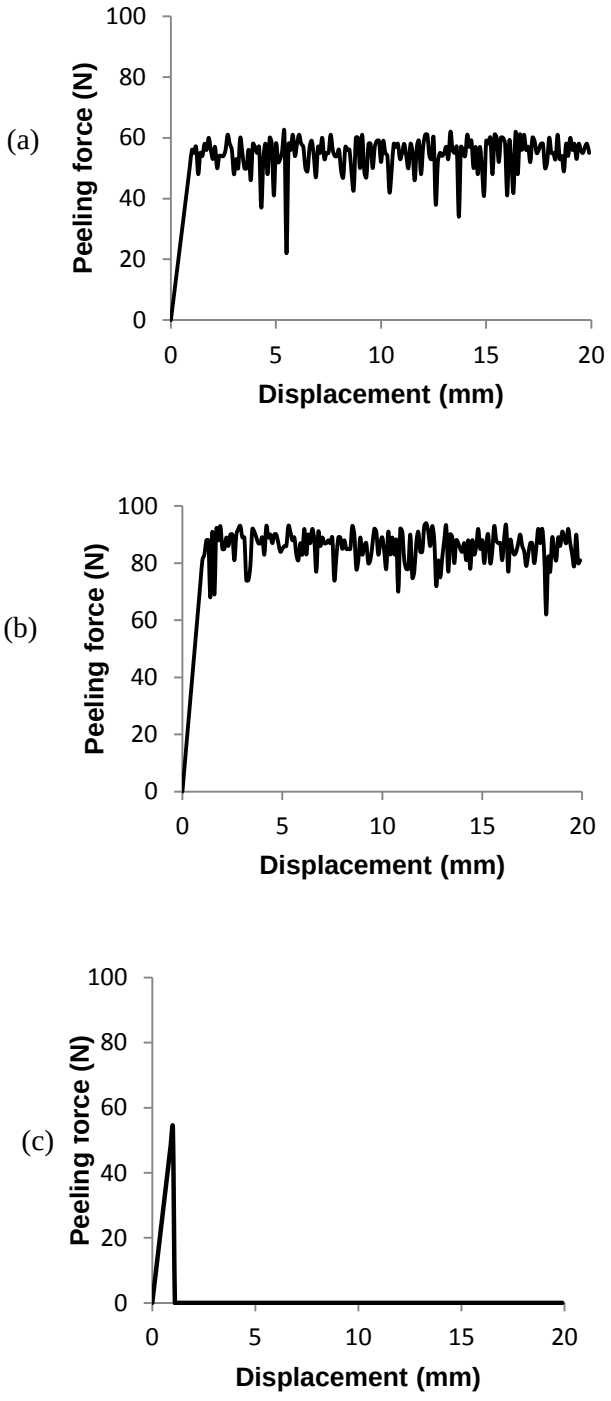

Figure 3.10. Simulated peeling forces for different scenarios: (a) F=50, U=15, G=20; (b) F=50, U=2, G=20; (c) F=10, U=15, G=20.

3.4.2.3 Model Parameter Adjustment

The results of the peeling test were used to determine the parameters, F, C and G for hemp. As only one parameter could be determined, one had to make assumptions for the other two parameters. The only form of peeling observed during the peeling test was the behaviour described as scenario (a), clean peeling, therefore, the coefficients of cohesive energy for the fibre, F, and core, U, were assigned a large value of 1000 J m^{-2}. This value serves the purpose of ensuring that neither fibre breaking nor core pull out will occur as the simulation took place. With this assumed value for F and U, the value of G was determined though matching the average forces measured in the peeling tests and those simulated using the model.

Since the available data for the peeling test did not yield differences between retting conditions, the value of G was only adjusted to account for differences between hemp varieties. Through trial and error method, the G values of 352 and 200 J m^{-2} result in the best match between the measured and simulated forces for USO 14 and Alyssa respectively. With these coefficients of adhesive energy, the resulting output of the stochastic model is presented in Figure 3.11. The stochastic model produced average peel forces of 0.86 N for USO 14 and 0.39 N for Alyssa.

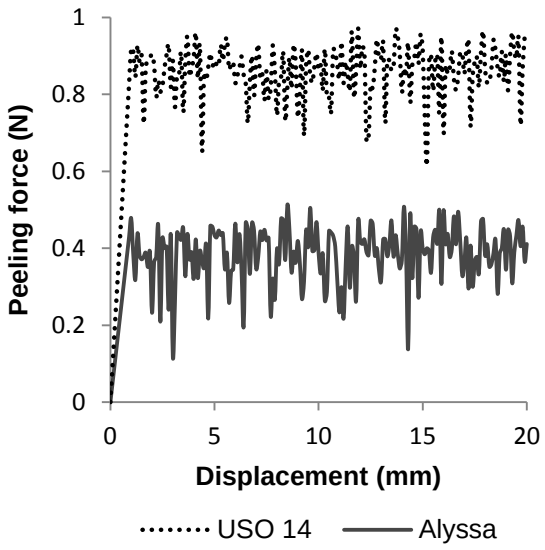

Figure 3.11. Stochastic model peeling force output.

Overall, the results of the stochastic model for fibre peeling were in accordance with the analysis of the peeling test, which further validated the application of the proposed method. Future research could potentially investigate magnitudes for the input parameters for a larger array of varieties and retting conditions. This would provide industry and researchers additional tools to compare the energy requirements of hemp-fibre separation as well as benefit the future design of decorticators for hemp. The versatility of this method could potentially be applied in researching energy requirements for peeling other types of natural fibres, such as flax, or to create mathematical models describing the energy required to break bonds uniting natural fibres to resins in a pull out test.

3.5 Conclusions

The peel test evaluating the strength required to separate the hemp fibre and core components was successfully conducted. The peeling forces and work required to peel hemp fibre were significantly different between the two hemp varieties tested, but not between the retting and unretting conditions. The average peeling force of fibre was 0.39 N, for Alyssa, and 0.86 N, for USO 14. The peeling force of hemp fibre was successfully simulated by the proposed stochastic model. The model was accurate in describing the behaviour observed during the peel tests, where the peeling force reached a peak value followed by a load oscillation approximate to an average value until the test was completed. Model parameters can be easily adjusted to model peeling of different hemp varieties and retting conditions. Additionally, this approach could potentially be applied to describe other material behaviours under conditions similar to those observed in a pull out test.

3.6 References

ASTM Standards. 2004. Standard Test Method for 90 Degree Peel Resistance of Adhesives. D6862. West Conshohocken, PA: ASTM.

Baker M. 2009. Evaluation of a Hammer Mill and Planetary Ball Mill for Hemp Fibre Decortication. Unpublished. M. Sc. Thesis. Winnipeg MB: Department of Biosystems Engineering, University of Manitoba.

Booth I., A.M. Goodman, R. J. Harwood and S.A. Grishanov. 2004. A mechanical investigation of the retting process in dew-retted hemp (Cannabis sativa). *Annals of Applied Biology* 145 (1):51-58.

Brook G., K. Liljefors, D. Brook, and A. Stewart. 2008. National industrial hemp strategy. Prepared for: Manitoba Agriculture, Food and Rural Initiative (2008 03 30). 358 p.

Bundy K. 2000. An improved peel test method for measurement of adhesion to biomaterials. *Journal of Materials Science: Materials in Medicine* 11 (8):517-521.

Franck R. R. 2005. *Bast and Other Plant Fibres*. Textile Institute. Manchester, England. CRC Press LLC. 397 p.

Goodman A. M., A. R. Ennos and I. Booth. 2002. A mechanical study of retting in glyphosate treated flax stems (Linum usitatissimum). *Industrial Crops and Products* 15 (2):169-177.

Hadavinia H., L. Kawashita, A. J. Kinloch, D. R. Moore and J. G. Williams. 2006. A numerical analysis of the elastic-plastic peel test. *Engineering Fracture Mechanics* 73 (16):2324-2335.

Inoue M. and K. Suganuma. 2009. Influential factors in determining the adhesive strength of ACF joints. *Journal of Materials Science: Materials in Electronics* 20 (12):1247-1254.

Von Maubeuge Kent P. and Ehrenberg H. 2000. Comparison of peel bond and shear tensile test methods for needlepunched geosymthetic clay liners. *Geotextiles and Geomembranes* 18:203-214.

Xie M. and V. M. Karbhari. 1998. Peel test for characterization of polymer composite/concrete interface. *Journal of Composite Materials* 32 (21): 1894-1913.

Yeomans, J. M. 1992. *Statistical Mechanics of Phase Transition*. New York: Oxford Science.

Zhong W., X. Ding and Z.L. Tang. 2001. Modeling and analyzing liquid wetting in fibrous assemblies. *Textile Research Journal* 71(9): 762-766.

Zhong W. and N. Pan. 2003. A computer simulation of single fiber pull out process in a composite. *Journal of Composite Materials* 37(21): 1951-1969.

Zhong W., N. Pan and D. Lukas. 2004. Stochastic modelling of tear behaviour of coated fabrics. *Modelling and Simulation in Materials Science and Engineering* 12(2): 293-309.

Chapter 4

Discrete Element Modelling of a Planetary Ball Mill

4.1 Abstract

The planetary ball mill is a versatile machine which has been used for grinding different types of materials for size reduction and lately for hemp decortication. A discrete element model (DEM) of a planetary ball mill was developed to predict the power and energy requirement of grinding hemp for fibre. Model development was facilitated through a series of grinding tests, which were performed on hemp using a planetary ball mill to examine the power draw of the mill. The test results identified that only grinding speed has a significant effect on the power draw. Power draw measurements, for grinding speeds of 200 – 500 rpm, ranged from 80 to 200 Watts with the power draw linearly increasing at greater grinding speed. The calibrated DEM was able to predict the power with relative errors of 0.31 to 28.2% when compared to the test results. The average value of kinetic energy predicted from the model, for grinding speeds of 200 – 500 rpm, ranged between 0.01 and 0.07 J per grinding ball. The DEM predicted that frictional power losses dispersed approximately 10% of the total power. Overall, the DEM improved understanding about the dynamics of the grinding balls within a planetary ball mill as well as the energy available for transfer in collisions between the grinding balls and hemp material.

Keywords: Discrete Element Model (DEM), Hemp, Planetary Ball Mill, Power, Energy, Kinetic, Friction

4.2 Introduction

The public has become concerned about environmental problems arising from unsustainable practices from using non-renewable materials. Hemp (*Cannabis sativa* Linnaeus) fibres are among various natural fibres that are considered to be an attractive material for use in the development of environmentally friendly and sustainable products (Kymäläinen and Sjoberg 2008; Hepworth et al. (2000a, 2000b)). A crucial step in obtaining hemp fibre is decortication, a mechanical process of extracting raw hemp fibres. Decortication of hemp is an energy intensive process because hemp plants possess a high percentage of cellulose and lignin (Bócsa and Karus 1997). Commonly used decortication equipment for hemp includes hammer mills, cutter heads, and roll crushers. Each piece of decortication equipment operates under slightly different principles involving the application of forces to hemp stalk to obtain the fibre (Fürll and Hempel 2000; Gratton and Chen 2004). All of these machines have multiple rotating parts, such as shafts and bearings of multiple types, which are in contact with hemp, causing hemp fibre wrapping around these rotating parts (Hobson et al. 2001; Dietz 1999). Hence, an operational limitation of these machines is the need for frequent stops to remove wrapped fibres and prevent any potential damage to the machines.

Alternatively, ball milling has great potential as effective decortication equipment. Overall, ball mills were able to defibrillate fibrous materials as well as improve fibre quality and fineness by applying impact and shear forces (Prasad et

al. 2005). The main advantage of this decortication method is that fibres are not in contact with any rotating machine parts. Hence, fibre wrapping problems and damage to rotating machine parts are no longer a concern. Previous studies by our research group have demonstrated promising potential of ball milling for hemp decortication (Baker et al. 2010) and for hemp fibre refining (Khan et al. 2009). However, in those studies, power requirement of ball milling was not investigated. Power requirement is an important performance indicator for any milling equipment, as milling is an energy intensive process (Yu et al. 2006; Lopo 2002; Shi et al. 2003).

The focus of this study was to investigate energy or power requirement by a particular type of ball mill known as the planetary ball mill for decorticating hemp. Planetary ball mills are well suited for laboratory-scale processing of materials in diverse industries (Rosenkranz et al. 2011). A future objective of industry is to develop large-scale units for industrial manufacturing purposes. The working principle of a planetary ball mill is based on the movement of a grinding bowl, filled with grinding balls. The grinding balls are subjected to superimposed rotational movements. The difference in speeds between the grinding balls and grinding bowl produces an interaction between frictional and impact forces, which releases high dynamic energy. The interaction between these forces results in extensive and highly effective energy transfer to the sample material (Lynch and Chester 2005).

The study of energy requirement also provides valuable information about energy transfer mechanisms acting within the planetary ball mill. The information about energy transfer mechanisms include power requirement, kinetic energy, and frictional power loses. Inside a planetary ball mill, multiple collision events transfer impact energy from the grinding balls to the hemp sample. The energy available for all collision events is provided by the movement of the grinding bowl, which is driven by an electric motor. Hence, there is a direct relationship between the total power draw of the mill and impact energy of the grinding balls. Since direct observation by means of on-line sensors is impractical, the next best option is numerical simulation (Mishra 2003a). One of the most effective methods of approximating the behaviour of individual particles (e.g. grinding balls) is using a discrete element model (DEM). A DEM consists of a time-stepping algorithm that requires three main elements: the repeated application of Newton's second law of motion to each particle (grinding ball) inside the considered system (grinding bowl); a force–displacement law to each contact; and a constant update of particle (grinding ball) and wall (grinding bowl) positions (Rosenkranz et al. 2011). The DEM has been successful at approximating ball milling internal behavior and motion patterns (Cleary and Hoyer 2000; Sato et al 2010; Radziszewski 2002; Rosenkranz et al. 2011).

In summary, although decortication and post-decortication using ball milling has been previously studied, information regarding energy requirements and dynamic behaviour of grinding balls in a planetary ball mill is scarce. Hence, the

objectives of this study were to: 1) develop a discrete element model to simulate decortication through a planetary ball mill; 2) calibrate the proposed model with experimental data; and 3) simulate dynamic behaviours of grinding balls inside the mill.

4.3 Experimental Study

4.3.1 Materials and Methods

4.3.1.1 Equipment

A planetary ball mill (FRITSCH PULVERISETTE 6 classic line, Idar-Oberstein, Germany) was used for grinding hemp to measure the power requirement of the mill. The machine consisted of a cylindrical grinding bowl with an inner diameter of 74.5 mm and a height of 86.7 mm (Fig. 4.1a). The effective volume of the bowl was 250 ml. The grinding media consisted of 15 spherical balls (Fig. 4.1b) with a 20-mm diameter. The balls were made of agate with a density of 2650 kg/m^3. The inside of the bowl had an agate liner. Thus, the interaction between the bowl and balls was agate to agate. The bowl was fixed on a support disc (Fig. 4.1c) and the distance between the axle of the bowl and the axle of the support disc was 62.5 mm. The mill was powered by a 1.1 kW electric motor. The bowl rotated about its own axis in one direction and also rotated with the support disc in the opposite direction. The relative speed ratio of the bowl to the supporting disc was 1.82. For every full rotation of the disc, the grinding bowl rotates 1.82 times about its own center in the opposite direction.

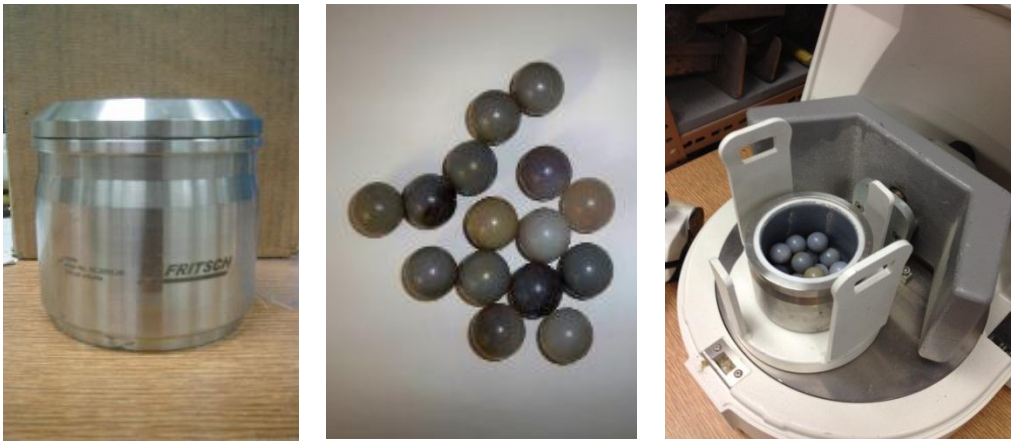

(a) (b) (c)

Figure 4.1. Principal components of a planetary ball mill: (a) grinding bowl; (b) grinding balls; (c) relative position of the grinding bowl on the supporting disc.

4.3.1.2 Hemp Sample Preparation

A test of hemp grinding was performed using the planetary ball mill. The hemp (variety: USO 31) was locally grown. Hemp samples were taken from bales which were stored to air dry to a moisture content of approximately 10%. Before being ground, hemp samples were cut into 40-mm segments so that they could fit into the grinding bowl.

4.3.1.3 Grinding Tests

The magnitude of the power requirement for grinding was expected to be affected mainly by the mill speed. A range of different grinding speeds was selected: 200, 300, 400, and 500 rpm according to the operational specifications of the mill. Power requirement may also change over time while a hemp sample is being ground, as the hemp particle size changes over time. Therefore, grinding

tests were performed for three different grinding durations: 3, 5, and 8 minutes. This gave a total of 12 combinations (4 speeds x 3 durations).

4.3.1.4 Test Procedure

The grinding bowl was filled with an approximately 6 g of randomly selected hemp sample for each test. Milling was initiated after the grinding bowl was secured to the support disc. Once the supporting disc and the grinding bowl started rotating, the grinding balls were subjected to superimposed rotational movements. The hemp material was impacted by the grinding balls, which resulted in separating of the fibre. The energy consumption in the grinding process was measured with a watt-hour meter directly connected to the ball mill; the watt-hour meter measured the power draw, in Watts, and the average power draw was recorded for each test. Each power draw measurement consisted of 15 readings from the watt-hour meter. Before each test, the power consumption without hemp was recorded for 5 minutes. Comparison of the energy consumption under both conditions, with and without samples, served as a means to determine the net power draw due to the presence of the hemp sample.

4.3.2 Results and Discussion

The impact forces applied by the planetary ball mill fragmented the hemp samples and separated fibre from the hemp stalk, which further supported the case for the use of ball milling in hemp decortication. The effects of different operational

conditions (grinding speed and duration) on power draw are discussed in this section.

4.3.2.1 Net Power Draw

The difference between power draw measurements, with and without hemp samples, was used to calculate the net power draw required to grind the samples. The average values of net power draw were very low, ranging between 0 and 3 Watts, which was only approximately 1 – 5% of the total power draw measured. A paired t-test showed that the differences in draw power were insignificant between the conditions with and without hemp sample in the bowl. In addition, the net power data had no particular trends, in terms of effects of grinding speed and duration. Although the hemp sample occupied a significant volume inside the grinding bowl, it did not affect the power required to operate the mill. A possible explanation is that the hemp sample possessed a relatively small mass, 6 g versus 165 g of grinding balls. The tests demonstrated that grinding media (balls) and its dynamics were the major factors affecting the power draw of ball milling.

4.3.2.2 Total Power Draw

Given the facts of the low net power draw and the insignificant differences between tests with hemp and without hemp, the total power data pooled from the tests with hemp and without hemp were used to examine effects of grinding speed. The effect of grinding speed on the power draw was quite significant (figure 4.2a and 4.2b). Milling at larger rotational speeds required increasing amounts of input power. The relationship between the power draw and rotational speed could be

described as a linear relationship with a coefficient of determination of 0.99. The results showed that the effect of grinding duration on the power draw measurements with hemp samples was insignificant. At 400 rpm, power draw was determined as 151 ± 6, 152 ± 7, and 153 ± 9 Watts for 3, 5, and 8 minutes respectively. All other grinding speeds followed a similar pattern, with average power draw values remaining approximately equal for different grinding durations (3, 5, and 8 minutes). Visual observations indicated that the milled materials differed in particle sizes between the different durations, as reported by Baker et al. (2010). However, this did not cause any changes on the power required to operate the mill.

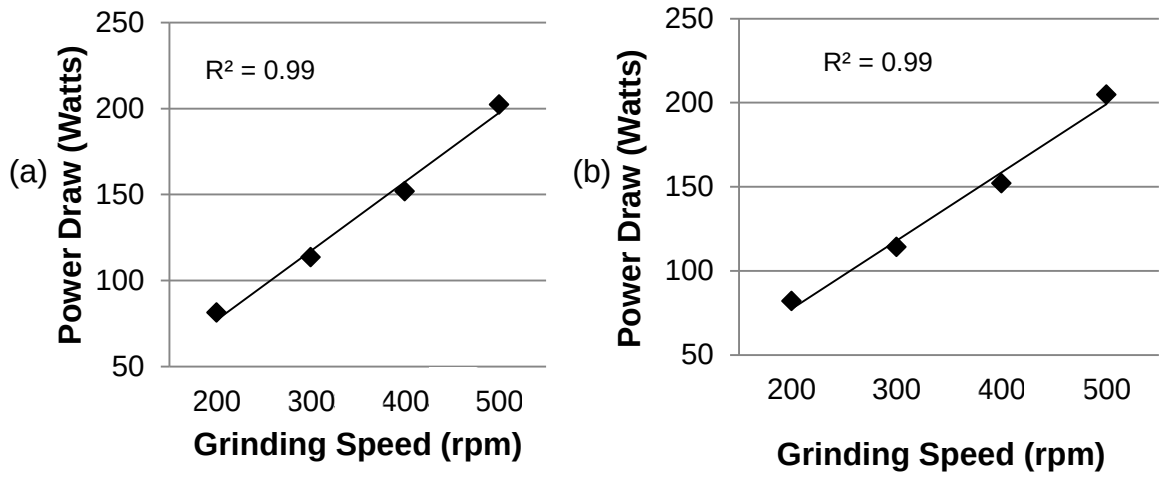

Figure 4.2. Power draw of the planetary ball mill: (a) Effect of grinding speed with samples; (b) Effect of grinding speed without samples.

4.4 Discrete Element Model

The test results demonstrated that the addition of hemp material and grinding duration did not affect the power draw. This information provided the base for the development of a simple but representative discrete element model (DEM) to simulate the planetary ball mill.

4.4.1 Model Development

4.4.1.1 Model of the Planetary Ball Mill

All the dimensions and properties of the ball mill within the model were equivalent to those of the previously described planetary ball mill. The planetary ball mill was modeled using the discrete element code PFC^{3D} (Figure 4.3). The main component of the model was the assembly of grinding balls which were represented by the PFC^{3D} basic spherical particles. Fifteen of those balls were enclosed inside a bowl which was constructed using a PFC^{3D} cylindrical wall as the body of the bowl and two flat square walls as the bottom and top covers of the bowl. The largest disc in Figure 4.3 functions as the supporting disc. The supporting disc provided a reference point to visualize the radius of the displacement of the grinding bowl. The medium-sized disc shown in Figure 4.3 is the grinding bowl support and it was used to ensure that the distance between the center of the bowl and the center of the support disc was constant at all times. Before running the simulations, a detailed examination was performed to ensure the right relative motion and position between the bowl and disc. This was done

through monitoring the position of the grinding bowl with a tracking particle following the same motion pattern as the grinding bowl support. The tracking particle was located in the center of the grinding bowl and it was positioned in such a way that it would not interact with the grinding balls inside the grinding bowl.

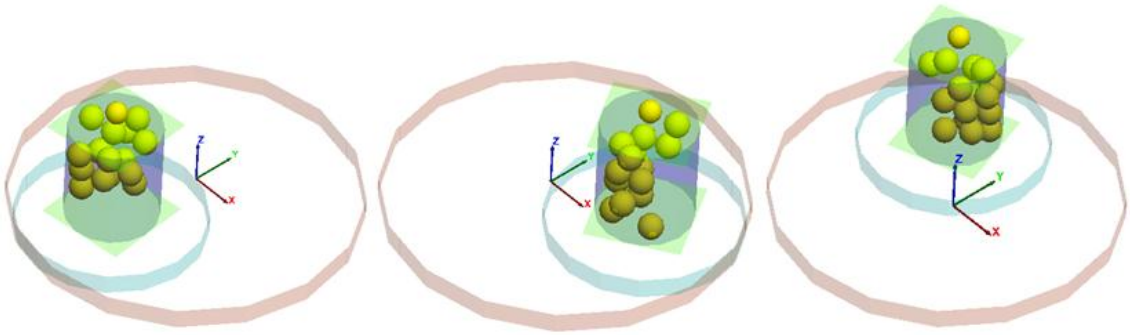

Figure 4.3. Screenshots of the model planetary ball mill at different simulation time steps.

4.4.1.2 Motion Generation

Figure 4.4 shows a simplified diagram of the relative motion of the grinding bowl with respect to the supporting disc. The rotational speed of the supporting disc, ω, was an adjustable variable in the simulation and was assigned values corresponding to the experiment. As described earlier, the angular velocity of the grinding bowl about its own center, β, was given by:

$$\beta = -1.82\,\omega \tag{1}$$

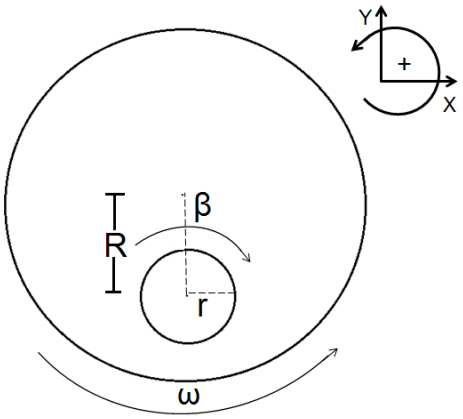

Figure 4.4. Motion diagram of the planetary ball mill (R = distance from the center of the grinding ball to the center of the grinding bowl; r = Radius of grinding bowl; ω = Angular velocity of supporting disc; β = Angular velocity of the grinding bowl).

The motion produced by the supporting disc was modeled as a function of ω and time. The absolute linear velocity, *V*, of the center of the grinding bowl with respect to the center of the supporting disc was given by:

$$V = R\omega \tag{2}$$

where *R* was the distance from the center of the grinding bowl to the center of the supporting disc (m) and ω was the constant angular velocity of the supporting disc (rad/s).

Although the simulation was coded in three dimensions, the function for circular displacement of the grinding bowl about the center of the supporting disc was categorized as two-dimensional motion parallel to the plane of the supporting disc. Therefore, the function for circular displacement was obtained by breaking the

absolute linear velocity into two vector components, V_x and V_y. The magnitude of these vector components was given as a function of the time required to complete one full revolution with boundary conditions as illustrated in Figure 4.5.

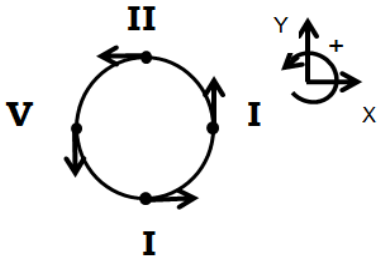

	I	II	III	IV
V_x	V	0	-V	0
V_y	0	V	0	-V

Figure 4.5. Boundary conditions for vector components of the linear velocity.

The equations for the vector components of the absolute displacement velocity were derived as:

$$V_x = \cos\left(\frac{\pi}{2t_{1/4}}\ t\right) V \tag{3.a}$$

$$V_y = \sin\left(\frac{\pi}{2t_{1/4}}\ t\right) V \tag{3.b}$$

where $t_{1/4}$ was the time required to complete one quarter of a revolution, in seconds. The value of $t_{1/4}$ was fixed depending on the magnitude of the rotational speed of the supporting disc. The variable t was the total accumulated time of the model, which started at zero and increased with each time step in the same units

as $t_{1/4}$. The value of $t_{1/4}$ was derived directly from the number of revolutions per minute, n, as:

$$t_{1/4} = \frac{15}{n} \tag{4}$$

Application of the previously described boundary conditions produced the desired motion within the model. The proposed system of equations worked for any assigned speed, while maintaining the same geometrical relationships found in the planetary ball mill. Figure 4.6 shows the displacement velocities of the center of the grinding bowl with respect to the center of the disc. Simultaneously, the grinding bowl constantly rotated about its own center at an angular velocity equivalent to β.

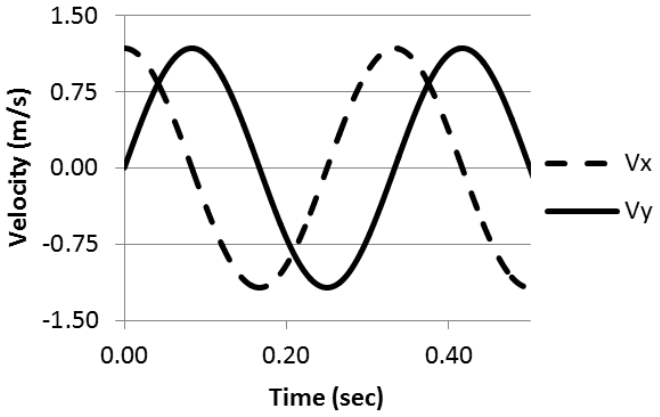

Figure 4.6. Change in velocity components over time at 200 rpm.

4.4.1.3 Model Parameters

Accurate material properties combined with different operating parameters yield useful predictions about equipment performance (Mishra 2003b). The

integration of DE equations required parameters which describe the contact nature between balls and between balls and the surrounding environment (bowl). The application of specific contact models was discussed in the work of Mishra (2003b) and had two basic models: the linear model to the Hertzian-type model. The linear-contact model is more suitable for the purposes of this study dealing with the interactions (ball-to-ball and ball-to-wall). The linear model is defined by the normal and shear stiffness, K_n and K_s, of the two contacting entities (ball-to-ball and ball-to-wall) (Itasca 2008). These parameters can be determined using Young modulus and Poisson's ratio of material (Cundall & Strack, 1982; Chang et al. 2003). In the developed DE model, the normal stiffness applied to the model was derived from the following relationship (Itasca 2008):

$$K_n = 4R_p\bar{E} \tag{5}$$

where K_n is the normal stiffness, R_p is the ball radii and E is the apparent young's modulus. Furthermore, the shear stiffness, K_s, was assigned the same value as the normal stiffness, K_n (Asaf et al. 2007; McDowell and Harireche 2002). The grinding balls and the walls within the model were assigned contact properties that were equivalent to Agate stones, with a density of 2650 kg/m^3 and a modulus of elasticity of 70 GPa (Fossen 2010). Application of the relationship in equation (5) resulted in a normal stiffness, K_n, value of 2.8x10^9 N/m. The values of all model parameters are summarized in table 4.1.

Table 4.1. DEM parameters applied to simulation.

Model parameter	Value
Ball density	2650 kg/m^3
Ball diameter	20 mm
Number of balls	15
Ball normal and shear stiffness	2.8x10^9 N/m
Ball to ball friction	0.3

4.4.1.4 Damping Coefficient

In DE models, energy supplied to the particles needs dissipation with damping mechanisms to arrive to a steady state solution (Itasca 2008). The PFC^{3D} code was able to dissipate kinetic energy with two types of damping, local and viscous damping. Local damping (*Ld*) applied a damping force to each ball, while viscous damping applied the damping force to each contact (ball-ball or ball-wall), which acted to oppose motion and dissipated the kinetic energy of particles in contact. Viscous damping had two damping components, normal (Vd_n) and shear (Vd_s). As a general rule of thumb, local damping was most appropriate for compact assemblies while viscous damping was preferred for situations involving free flight of particles or impacts between particles. The planetary ball mill was subject to both scenarios because it behaved as a compact assembly at low grinding speeds but particles took flight and collided at higher grinding speeds. The combination of these two types of damping provided the most accurate physical representation of

the ball assembly. The damping coefficients are crucial to the model, and they needed to be calibrated.

4.4.2 Calibration of Damping Coefficient

The damping coefficients (Ld, Vd_n, and Vd_s) were calibrated using the power draw data from the tests. The calibration process is described in the following sections.

4.4.2.1 Model Prediction of Power

The model was used to predict the power required for moving the grinding balls inside the bowl. This power is equivalent to the total accumulated work of the walls (i.e. the grinding bowl) on the assembly of balls. The PFC^{3D} is able to monitor this work which is defined as:

$$E_w = \sum_{Nw}(F_i \Delta U_i + M_i \Delta \theta_i) \quad (6)$$

where E_w is the total accumulated work of the wall; N_w is the number of walls (one cylindrical wall and two flat walls in this case); F_i and M_i are the resultant force and moment acting on the wall; and U_i and θ_i are the applied displacement and rotation. Under the assumption that all the energy provided to the systems originated from this source, the power was calculated through the magnitude of E_w divided by the total accumulated time. The magnitude of E_w was positive or negative, with the convention that work of the walls on the particles is positive.

Preliminary simulations demonstrated that as the damping coefficients were adjusted, dissipation of more energy due to damping would cause lower magnitudes of the power predicted by the model. An example of this type of behavior is present in Figure 4.7, in which every parameter remains constant with the exception of two damping coefficients. It was clear that the damping coefficients significantly affect the model outputs both over time and in magnitude. Dynamic behaviours of the ball assembly were very sensitive to the input viscous damping coefficients.

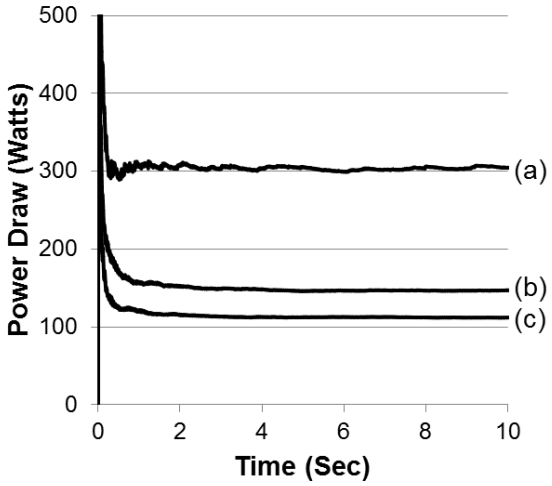

Figure 4.7. Effect of damping coefficient on power draw at 400 rpm: (a) *Ld*=0.4, Vd_n=0, Vd_s=0; (b) *Ld*=0.4, Vd_n=0.3, Vd_s=0.3; (c) *Ld*=0.4, Vd_n=0.6, Vd_s=0.6 (*Ld*= Local damping; Vd_n= Viscous normal damping, Vd_s= Viscous shear damping).

4.4.2.2 Power Comparisons between Simulations and Measurements

The measured power draw was the total energy introduced into the planetary ball mill from the electricity source. The difference between the measured

power draw and the simulated power was that the measured power included the mechanical losses in the process of transmitting electricity energy to the ball assembly. The mechanical loses were assumed as 10% of the required power draw (Wills 1979). Thus, the measured power draws were reduced by 10% before being compared with the powers predicted by the model.

The power was simulated for multiple combinations of Ld, Vd_n, and Vd_s at different grinding speeds (200, 300, 400, and 500 rpm). The results showed that changes in Ld had little influence in power draw after the grinding balls engaged in free flight, whereas changes in Vd_n and Vd_s had significant effects in the power with larger Vd_n and Vd_s required for faster grinding speeds. There was not a single combination of Vd_n and Vd_s that would accurately approximate the power draws measured for all grinding speeds. For example, with a set of Vd_n and Vd_s, the predicted value of power for the 200 rpm was comparable to the measurements, but that for the 300 rpm had a relative error of over 40% when compared to the measurement, which was not adequate for approximating the actual power draw in the planetary ball mill. It was recognized that the Vd_n and Vd_s were grinding speed dependent rather than constant through grinding operations. Hence, a specific set of Vd_n and Vd_s was required for each grinding speed.

Therefore, simulations were performed to calibrate the damping coefficients separately for different grinding speeds. For simplicity, values of Ld was kept constant for the different grinding speeds and values of Vd_n and Vd_s were kept the

same for each speed. During the calibration of each speed, the model was run to simulate the power of the ball mill, and the input damping coefficients were being adjusted until the simulated power matched the experimental data. It was found that a constant value (0.4) was an adequate *Ld* for all speeds. The calibrated values of Vd_n and Vd_s were increased as the grinding speed increased, which represented the slowing down of grinding balls. The calibrated results with the lowest relative errors are shown in table 4.2. The average relative errors for the speeds of 200, 300, and 400 rpm were all below 10%, which indicated that the model was able to adequately approximate power draw. However, the relative error for the 500 rpm was 28.2%, which is quite high.

Table 4.2. Calibrated damping coefficients for different mill speeds.

Speed (rpm)	Damping Coefficient			Power (Watts)		Relative Error (%)
	Ld	Vd_n	Vd_s	Model	Test	
200	0.4	0	0	81.6	81.4	0.31
300	0.4	0.3	0.3	102	114	9.96
400	0.4	0.6	0.6	147	152	3.19
500	0.4	1.2	1.2	264	204	28.2

4.4.3 Model Simulations

The calibrated model was used to simulate dynamic behaviours of the ball assembly. The PFC^{3D}-EV (Enhanced Visualisation) used in this study enables the user to obtain many dynamic attributes of the balls. This study focused on the kinetic behaviours of the ball assembly. Movement of the grinding balls within the

ball mill led to collisions, which became the main mechanism transferring energy from the grinding balls to the hemp sample. Simulations also focused on the friction energy loss of the assembly of balls. A portion of the power introduced into the system was dispersed as frictional energy. All simulations were performed under different grinding speeds using the calibrated damping coefficients listed in Table 4.2.

4.4.3.1 Motion Pattern of the Balls

Visual representation of grinding ball motion within the planetary ball mill was possible through the simulations. Figure 4.8 provides an example of monitoring grinding balls to determine their locations after one full revolution. The grinding balls followed a cascading type of motion for the proposed range of grinding speeds. The grinding balls were “flying” towards the opposite end of the cylinder wall. Through enhanced understanding of motion patterns, the DE model enabled future study of design factors such as the operational grinding speed, sizes of the grinding balls and bowl, friction coefficients, and the ratio of material to bowl volume. These design factors have a direct effect in the effectiveness and location of the grinding areas where high impact forces decorticate the hemp sample.

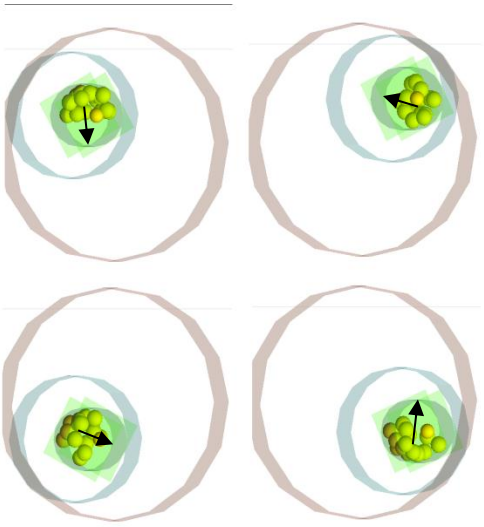

Figure 4.8. Screenshot of grinding ball motion pattern after one full revolution of the grinding bowl.

The monitoring of the velocity distribution within grinding balls helps supplement grinding ball position information. The proposed DEM was able to record the translational velocity distribution at different grinding speeds. The velocity distribution (Figure 4.9) indicates that grinding balls adjacent to the bowl wall have a different translational velocity than those closer to the center of the grinding bowl. The differences in translational velocities were in the order of 0.5 m/s, which support the argument for calculating the average kinetic energy of each ball as the average kinetic energy within the model.

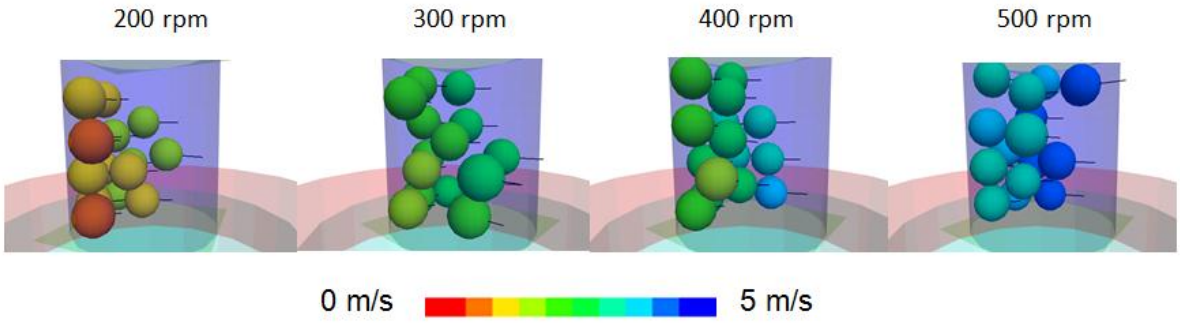

Figure 4.9. Velocity distribution of grinding balls at different grinding speeds.

4.4.3.2 Kinetic Energy of the Balls

Previous studies (Magini et al. 1996; Iasonna and Magini 1996; Abdellaoui and Gaffet 1995) determined collision energy by linking it directly to the kinetic energy of each individual grinding ball. The collision energy in the planetary ball mill was assumed equivalent to the total kinetic energy of the balls' motion. The proposed model was able to determine the total kinetic energy, E_k, of all particles accounting for both translational and rotational motion as (Itasca 2008):

$$E_k = \frac{1}{2}\sum_{Nb}(m_i V_i^2 + I_i \omega_i \cdot \omega_i) \quad (7)$$

where Nb, m_i, I_i, V_i and ω_i are, the number of balls, inertial mass, inertia tensor, and translational and rotational velocities of ball i, respectively. The average kinetic energy provides information about the amount of energy available for transfer from the grinding balls into the hemp stems. Average kinetic energy was approximated for each ball from the division of the total kinetic energy by the number of grinding balls present in the model.

The average magnitude of the modeled kinetic energy, for each given grinding speed, consisted of slight diversions in magnitude about an average value. An example of the kinetic energy output from the model is shown in Figure 4.10, which includes the range of values of the total kinetic energy including all grinding balls at a grinding speed of 200 rpm for 10 seconds.

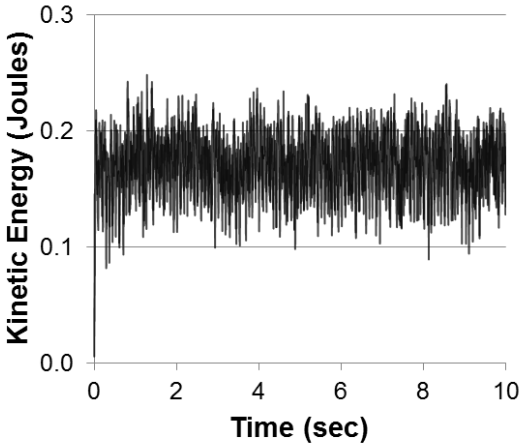

Figure 4.10. Total kinetic energy predicted by the model for the 200 rpm grinding speed.

The results obtained from the model were plotted in Figure 4.11. The curve approximates the average kinetic energy, in Joules, per ball at different grinding speeds. The order of magnitude of the predicted kinetic energy was in accordance with studies performed by Magini et al. (1996), who established that the collision energy of individual balls was in the order of 10^{-2} Joules per collision. The best fit curve of the data was found to follow a power relation with a coefficient of determination of 0.98. The predicted kinetic energy provided information about energy transferred from the grinding balls into the hemp sample during milling.

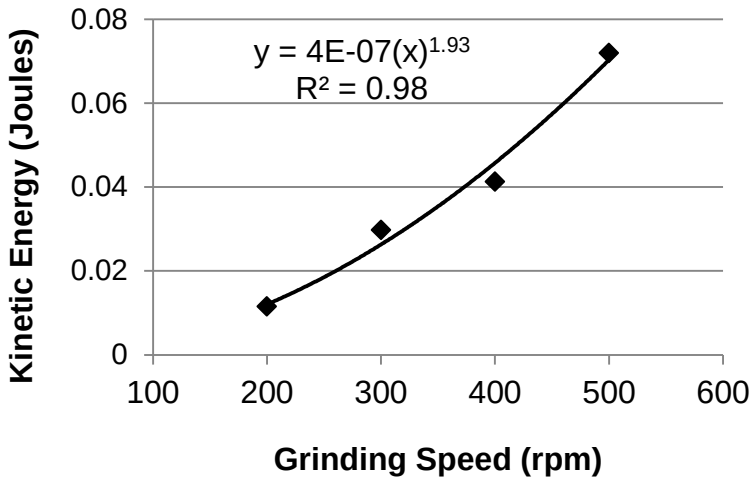

Figure 4.11. Average kinetic energy per ball at different grinding speeds.

4.4.3.3 Frictional Power Losses

Within the proposed model, the total accumulated frictional energy loses, E_f, was defined (Itasca 2008) as:

$$E_f = \sum_{Nc}(F_{is}\Delta U_{is}) \quad (8)$$

where Nc is the number of contacts; and F_{is} and ΔU_{is} are the average shear force and the increment of slip displacement. E_f represents the magnitude of the total accumulated energy dissipated through frictional sliding at all contacts. The total friction power losses were calculated from dividing the total energy dissipated through friction with the total accumulated time. Figure 4.12 shows a typical curve of friction loss over time.

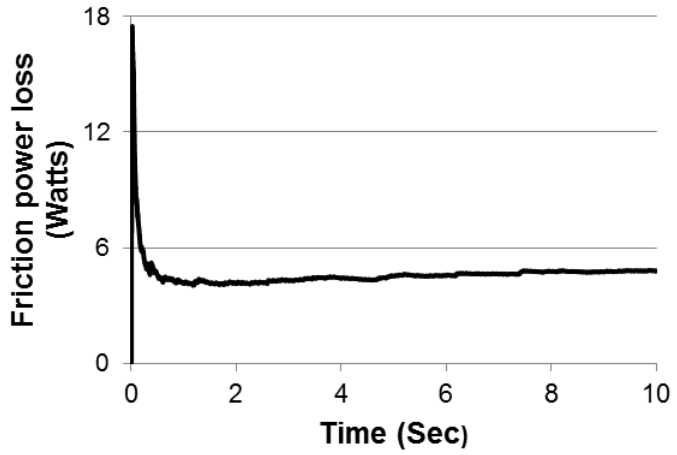

Figure 4.12. Friction power loss at 200 rpm.

The magnitude of the frictional power losses increased at larger grinding speeds (Figure 4.13). However, frictional power losses represented only a small percentage of the total power. The energy dispersed through friction at 200, 300, 400, and 500 rpm accounted for 5.7, 11, 11, and 13% of the total power respectively. In average, it was determined that approximately 10% of power was dispersed as frictional energy, which is representative of gradual contributions to the overall wear of the mill. After frictional losses, the remaining applied energy mostly in the form of kinetic energy driving high energy impacts during the milling process.

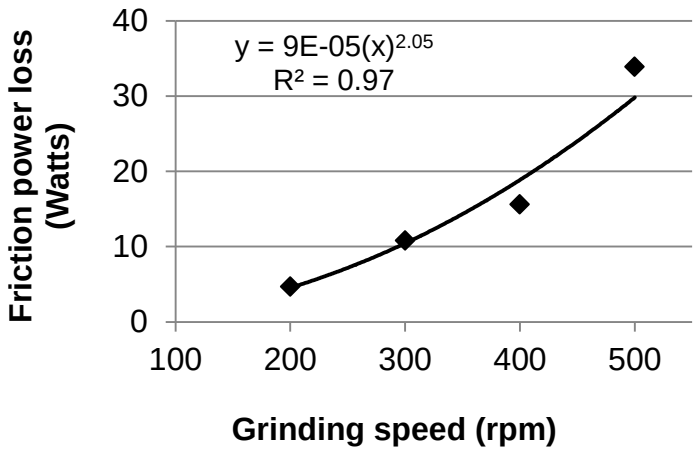

Figure 4.13. Friction power losses at different grinding speeds.

Although further experiments are required to determine the applicability of current model parameters to different types of milling arrangements, the DEM could potentially evaluate the effect of various conditions through changing the variables such as grinding media, grinding speed, and mill dimension. Hence, the proposed model improves our capacity to recreate and understand the dynamics inside a planetary ball mill.

4.5 Conclusion

Tests were performed with the intension of determining energy consumption of decorticating hemp using a planetary ball mill. The results showed that the energy consumption of milling hemp was attributable mainly to the grinding media, not the hemp being ground. The power draw of milling operation significantly varied with the grinding speed, not the grinding duration. The planetary ball mill was successfully modeled using a DEM with appropriate geometrical relationship of the

motion in the grinding bowl. It was found that damping coefficients were the most crucial model parameters in this application, and they are grinding speed dependent. The calibrated DEM would be suitable for mill speeds lower than 400 rpm. The model was able to simulate the kinetic energy and frictional power losses of the ball assembly of the mill. The simulation revealed that both the kinetic energy and friction power losses had a power relationship with the grinding speed.

The developed DEM will allow for future study of different model parameters, such as size and material of grinding media, mill dimensions, and grinding speeds. In addition to predict the kinetic energy and friction power losses, the model is able to analyse many attributes of a ball, such as the position, translational and rotational displacement, acceleration, number of contacts with neighbouring balls. This will provide valuable information about positioning of the different grinding zones within the planetary ball mill. These however were not within the scope of this study. Further experiments and research are required to evaluate the applicability of this approach for a different set of experimental conditions.

4.6 References

Abdellaoui M. and E. Gaffet. 1995. The physics of Mechanical Alloying in a Planetary Ball mill: Mathematical Treatment. *Acta Metallurgica et Materialia* 43(3):1087-1098.

Asaf, Z., D. Rubinstein and I. Shmulevich. 2007. Determination of discrete element

model parameters required for soil tillage. Soil & Tillage Research 92(2): 227–242.

Baker, M.L., Y. Chen, C. Lague, H. Landry, Q. Peng, W. Zhong and J. Wang. 2010. Hemp fibre decortications using a planetary ball mill. *Canadian Biosystems Engineering* 5:7-15.

Chang, C. S., C. L. Liao and Q. Shi. 2003. Elastic granular materials modeled as first order strain gradient continua. *International Journal of Solids and Structures* 40: 5565–5582.

Cleary P., and D. Hoyer. 2000. Centrifugal mill charge motion and power draw: comparison of DEM predictions with experiment. *International Journal of Mineral Processing* 59:131-148.

Cundall, P. A. and O. D. L. Strack. 1982. Modeling of microscopic mechanics in granular material. In: J. T. Jenkins, & M. Satake (Eds.), *Mechanics of Granular Materials: New Models and Constitutive Relations* (pp. 113–149). Amsterdam: Elsevier.

Dietz, J. 1999. Hemp growing pains. The Furrow.104:16-18.

Fossen H. 2010. Structural Geology, 1st edition, New York, USA: Cambridge University Press.

Fritsch GmbH. 2003. Planetary Mono Mill, “pulverisette 6” operating instructions manual. Industriestrasse, Idar-Oberstein: Fritsch GmbH.

Fürll, C. and H. Hempel. 2000. Effective processing of bast fiber plants and mechanical properties of the fibers. ASAE Paper No. 046091. St. Joseph, Mich.: ASABE.

Gratton, J.L. and Y. Chen. 2004. Development of a field-going unit to separate fibre from hemp (Cannabis sativa) stalk. *Applied Engineering in Agriculture* 20(2):139-145.

Hepworth, D.G; R.N. Hobson, D.M. Bruce and J.W. Farrent. 2000a. The use of unretted hemp fibre in composite manufacture. *Composites Part A - applied science and manufacturing* 31(11):1279-1283.

Hepworth, D. G., D.M. Bruce, J. F. V. Vincent, G. Jeronimidis. 2000b. The manufacture and mechanical testing of thermosetting natural fibre composites. *Journal of Materials Science* 35(2):293-298.

Hobson R.N., D.G. Hepworth and D.M. Bruce. 2001. Quality of Fibre Separated from Unretted Hemp Stems by Decortication. *Journal of Agricultural Engineering Research* 78(2): 153-158.

Iasonna A. and M. Magini. 1996. Power Measurements During Mechanical Milling. An Experimental way to Investigate the Energy Transfer phenomena. *Acta Metallurgica et Materialia* 44(3):1109-1117.

Itasca. 2008. Pfc^{3d} particle flow code in 3 dimensions, theory and background. Minneapolis, Minnesota, USA: Itasca consulting group, Inc.

Khan, M. R., Y. Chen, O. Wang and J. Raghavan. 2009. Fineness of Hemp (Cannabis Sativa L.) Fiber Bundle after Post-Decortication Processing Using a Planetary Ball Mill. *Applied Engineering in Agriculture* 25(6):827-834.

Kymäläinen, H.R. and A.M. Sjoberg. 2008. Flax and hemp fibres as raw materials for thermal insulations. *Building and Environment* 43: 1261-1269.

Lopo, P. 2002. The right grinding solution for you: roll, horizontal or vertical. *Feed Management* 53(3):23-26.

Lynch A. and, R. Chester. 2005. The History of grinding. Littleton, Colorado, USA: Society for Mining, Metalurgy and Exploration Inc.

Magini M., A. Iasonna and F. Padella. 1996. Ball Milling: an Experimental Support to the Energy Transfer Evaluated By the Collision Model. *Scripta Materialia* 34(1):13-19.

McDowell, G.R., Harireche, O., 2002. Discrete element modelling of yielding and normal compression of sand. Geotechnique 52 (4): 299–304.

Mishra B.K. 2003a. A review of computer simulation of tumbling mills by the discrete element method: Part I—contact mechanics. *International Journal of Mineral Processing* 71:73-93.

Mishra B.K. 2003b. A review of computer simulation of tumbling mills by the discrete element method Part II - Practical applications. *International Journal of Mineral Processing* 71:95-112.

Prasad, B.M., M.M. Sain and D.N. Roy. 2005. Properties of ball milled thermally treated hemp fibers in an inert atmosphere for potential composite reinforcement. *Journal of Material Science* 40(16):4271-4278.

Radziszewski P. 2002. Exploring total media wear. *Mineral Engineering* 15. 1073-1087.

Rosenkranz S., S. Breitung-Faes and A. Kwade. 2011. Experimental investigations and modelling of the ball motion in planetary ball mills. *Powder Technology* 212:224-230.

Sato A., J. Kano, F. Saito. 2010. Analysis of abrasion mechanism of grinding media in a planetary mill with DEM simulation. *Advanced Powder Technology* 21:212-216.

Shi, F., T. Kojovic, J.S. Esterle, D.David. 2003. An energy-based model for swing hammer mills. *International Journal of Mineral Processing* 71(1): 147-166.

Yu M., A. R. Womac, P.I. Miu, C. Igathinathane, S. Sokhansanj and S. Narayan. 2006. Direct Energy Measurement Systems for Rotary Biomass Grinder – Hammermill. In ASABE Annual International Meeting, 066217. Portland, Oregon. July 9-12.

Wills, B. A. 1979. Mineral Processing Technology : an Introduction to the Practical Aspects of ore Treatment and Mineral Recovery, 1St edition. Willowdale, Ontario: Pergamon Press.

Chapter 5
General Conclusions and Recommendations

The experiments described in Chapters 3 and 4 successfully measured the strength of the hemp fibre-core interface as well as the power draw required to decorticate hemp, respectively. Mechanical properties relevant to hemp processing were accurately approximated through two computer models: a stochastic model simulating fibre peeling behaviour, and a discrete element model simulating stress conditions inside a planetary ball mill.

There were significant differences in peeling strength between the USO 14 and Alyssa hemp varieties. Unfavourable weather conditions during dew retting are likely to have caused under-retting of the hemp stems. Hence, retting condition did not affect the peeling behaviour of the hemp samples in this study. The variation on the work to peel was large for the studied hemp varieties, which is consistent with findings documented for similar experiments with hemp. Processing varieties with such large variations in their mechanical properties creates challenging conditions for the production of materials with consistent properties. The peeling behaviour observed in both hemp varieties was stochastically modeled through simple adjustments in model parameters. Continuation of this research should focus on the assessment of mechanical properties for a wider range of hemp varieties, with the objective of identifying hemp varieties that are easier to decorticate and offer higher uniformity of fibre.

Power draw measurements increased linearly at larger grinding speeds of the ball mill. The mass of the processed hemp was relatively small as compared to the mass of the grinding balls. Hence, the net power draw for processing hemp was insignificant in this study, but this could change under the conditions of a large scale operation as the mass ratio of hemp to grinding media increases. The developed discrete element model approximated the power draw, and can predict dynamic behaviours of the balls inside the mill. Model results indicate that frictional losses accounted for approximately 10% of the total power. Kinetic energy predictions were in the same order of magnitude as analytical methods described in literature. Future studies involving changes in model parameters, such as size and composition of grinding media, mill dimensions, and grinding speeds, are recommended to assist the design of large-scale prototypes.

Both computer models complement each other and have the potential to enhance the way industry will approach the evolution of equipment for hemp decortication. The detailed study of hemp decortication equipment, such as planetary ball mills, will provide information about forces applied during the decortication process. Computer models such as the DEM described in chapter 4 will continue to enhance our understanding of the mechanisms in which energy is transferred to the decorticate hemp. Furthermore, the stochastic model could be implemented to determine optimal processing parameters based on simulated predictions of the peel strength of hemp.